

**VALIDATION OF THERMAL ENHANCEMENT IN MICRO
CHANNEL HEAT SINK USING NUMERICAL ANALYSIS**

QAMAR FAIRUZ BIN ZAHMANI

**FACULTY OF ENGINEERING
UNIVERSITY OF MALAYA
KUALA LUMPUR**

2018

**VALIDATION OF THERMAL ENHANCEMENT IN
MICRO CHANNEL HEAT SINK USING NUMERICAL
ANALYSIS**

QAMAR FAIRUZ BIN ZAHMANI

**RESEARCH REPORT SUBMITTED IN PARTIAL
FULFILMENT OF THE REQUIREMENTS FOR THE
DEGREE OF MASTER OF ENGINEERING
(MECHANICAL)**

**FACULTY OF ENGINEERING
UNIVERSITY OF MALAYA
KUALA LUMPUR**

2018

UNIVERSITY OF MALAYA
ORIGINAL LITERARY WORK DECLARATION

Name of Candidate: Qamar Fairuz Bin Zahmani

Matric No: KQK 160005

Name of Degree: Degree of Master of Mechanical Engineering

Title of Project Research Report: Validation of thermal enhancement in micro channel heat sink using numerical analysis.

Field of Study: Fluid dynamics and Heat Transfer

I do solemnly and sincerely declare that:

- (1) I am the sole author/writer of this Work;
- (2) This Work is original;
- (3) Any use of any work in which copyright exists was done by way of fair dealing and for permitted purposes and any excerpt or extract from, or reference to or reproduction of any copyright work has been disclosed expressly and sufficiently and the title of the Work and its authorship have been acknowledged in this Work;
- (4) I do not have any actual knowledge nor do I ought reasonably to know that the making of this work constitutes an infringement of any copyright work;
- (5) I hereby assign all and every rights in the copyright to this Work to the University of Malaya ("UM"), who henceforth shall be owner of the copyright in this Work and that any reproduction or use in any form or by any means whatsoever is prohibited without the written consent of UM having been first had and obtained;
- (6) I am fully aware that if in the course of making this Work I have infringed any copyright whether intentionally or otherwise, I may be subject to legal action or any other action as may be determined by UM.

Candidate's Signature

Date:

Subscribed and solemnly declared before,

Witness's Signature

Date:

Name:

Designation:

ABSTRACT

The cooling of electronic devices is essential to guarantee their functional performance and operational lifetime. Due to continued miniaturization and integration of transistors in packaged chips, the heat dissipation rate has surpassed the limits of classical air-cooled heat sinks. This has triggered a lot of research towards alternatives for high heat flux cooling. Liquid cooling with micro heat sinks is one of these candidate solutions. The first part of this thesis focusses on the validation of thermal enhancement in microchannel heat sink (MCHS) using numerical analysis. The single channel computational domain for the numerical simulation was adopted from MCHS. The basic geometry of the computational domain was obtained from the existing literature which related to the geometry of MCHS. With using experimental model demonstrated by M.R.Sohel, his experimental data was used as a reference to compare with the available analytical correlation and with numerical approached. The rate of heat transfer and flow of coolant of the MCHS in laminar or steady state condition were numerically investigated at a constant heat flux. Besides that, the study of the thermal and pressure loss's geometrical parameter effects will be carried out in this research. In the second part of this thesis, this there were an additional studied on the effect of aspect ratio and fluid flow rate in the MCHS, and the result obtained is discussed in this thesis. The overall result of the present work shows there is a close relationship between both the numerical and analytical data.

Keywords: Microchannel, Validation, Heat Transfer.

ABSTRAK

Penyejukan peranti elektronik adalah penting untuk menjamin prestasi fungsi dan operasi sepanjang hayat mereka. Disebabkan peminiaturan berterusan dan integrasi transistor dalam cip berbungkus, kadar pembebasan haba telah melebihi had pembenam haba sejukan udara yang klasik. Ini telah mencetuskan banyak penyelidikan ke arah alternatif untuk menyejukkan fluks haba tinggi. Penyejukan cecair dengan mikro pembenam haba adalah salah satu kaedah penyelesaian. Bahagian pertama tesis ini memfokuskan kepada proses pengesahan daripada peningkatan Pembenam Haba Saluran Mikro (MCHS) dengan menggunakan analisa berangka. Komputasi lingkungan saluran tunggal telah dipilih daripada model fizikal MCHS bagi simulasi yang berangka. Asas geometri komputasi lingkungan telah diambil dari geometri MCHS daripada kajian yang sedia ada. Dengan menggunakan model eksperimen yang ditunjukkan oleh M.R.Sohel, data eksperimen itu digunakan sebagai rujukan untuk membandingkan dengan hubung kait analisis yang sedia ada dan dengan kaedah berangka. Penyejuk aliran dan ciri-ciri haba yang dipindahkan melalui MCHS ini di selidik dalam keadaan lamina dan keadaan stabil pada fluks haba yang berterusan. Kesan kehilangan haba dan tekanan terhadap geometri juga dikaji. Dalam bahagian kedua tesis ini, terdapat satu kajian tambahan pada kesan nisbah dan kadar aliran bendalir di dalam MCHS, dan keputusan yang diperolehi dibincangkan dalam tesis ini. Hasil keseluruhan kerja semasa menunjukkan terdapat satu persetujuan yang baik untuk antara kedua-dua data berangka dan analisis.

Katakunci: Saluran mikro, Pengesahan, Pemindahan Haba.

ACKNOWLEDGEMENTS

Firstly, thanks to the Almighty Allah SW.T for giving me the opportunity to complete my study on time. I would also like to express my sincere gratitude to my Supervisor Associate Professor Ir Dr. Nik Nazri Nik Ghazali who accepted me as his research student and for his support of my degree project study. Even though he is currently serving as Vice Dean (HEP) for the faculty but the commitment and his patient guidance that helped me along the duration of completing this research study and the writing of this thesis.

Special thanks also to my fellow lab mates Mr. Zulhusni, my office mates Mr. Ir Hafiz, Mr. Azwar and Mr. Faruq for the time and helping me during completing this project and thanks to Universiti Teknikal Malaysia Melaka (UTeM) for sponsoring my degree study.

At last but not least, I would also like to thanks my beloved wife Mdm Siti Nor'ain Mokhtar and family member for supporting me and keeping me motivated in completing this degree. Not forget my lovely mother Mdm. Mariam Hj Rejab, whom always prays for my success in my study and in my life. This project is dedicated to her for ongoing love and support and to my lovely father (Arwah Mr. Zahmani Mohammad Ali) who could not see this Master project completed.

TABLE OF CONTENTS

Abstract	iii
Abstrak	iv
Acknowledgements	v
Table of Contents	vi
List of Figures	x
List of Tables.....	xii
List of Symbols and Abbreviations.....	xiii
List of Appendices	xv
CHAPTER 1: INTRODUCTION.....	1
1.1 Background.....	1
1.2 Problem Statement.....	2
1.3 Scope of Study.....	3
1.4 Objective of Study.....	3
1.5 Methodology.....	3
1.5.1 Model benchmark and analysis.....	4
1.5.2 Validation.....	5
1.6 Outline of the Thesis.....	5
CHAPTER 2: LITERATURE REVIEW.....	7
2.1 Introduction.....	7
2.2 Microchannel Concepts	7
2.3 Analytical Studies.....	9
2.4 Numerical Studies.....	15
2.5 Laminar and Turbulence Flow	17

2.6	Reynold Number.....	17
2.7	Boundary Layer	18
2.8	Boundary Layer Equations	19
2.9	Computational Fluid Dynamics (CFD)	19
2.10	FLUENT Overview	21
2.11	Navier-Stokes Equations	21
2.12	SIMPLE algorithm.....	22
CHAPTER 3: METHODOLOGY		24
3.1	Outline.....	24
3.2	Physical Model of Microchannel heat sink	26
3.3	Computational Grid for Solution Domain of the microchannel heat sink.....	28
3.4	Computation	29
3.5	Governing Equation.....	29
3.5.1	Fluid.....	29
3.5.2	Solid.....	30
3.6	Boundary Conditions	30
3.6.1	Thermal Boundary Conditions	30
3.6.2	Hydrodynamic Boundary Conditions.....	31
3.7	Solution Method	32
3.8	Mathematical Formulation.....	33
3.8.1	Thermal Characteristic	33
3.8.2	Fluid Characteristic	34
3.9	Finite Volume Method (FVM)	34
3.10	Numerical method and validation.....	35
3.10.1	Analytical and numerical analysis.....	35
3.10.2	Experimental analysis.....	36

CHAPTER 4: RESULTS AND DISCUSSION	38
4.1 Outline.....	38
4.2 Temperature Contour of Microchannel	39
4.3 Pressure contour of microchannel	41
4.4 Velocity Vector of microchannel.....	42
4.5 Grid independence study	43
4.6 Steinke & Kandlikar validation	44
4.7 Philips validation	45
4.8 Steike & Kandlikar and Sohel	46
4.9 Effect of aspect ratio.....	48
4.9.1 Variation between different Aspect ratio and Temperature different	49
4.9.2 Variation between Aspect Ratio and Thermal Resistance	50
4.9.3 Variation between Aspect Ratio and Heat Transfer Coefficient.....	51
4.9.4 Variation between Aspect Ratio and Nusselt number.....	52
4.9.5 Variation between different Aspect Ratio and Pressure Drop.....	53
4.9.6 Variation between different Aspect ratio and Pumping Power	54
4.10 Effect of Flow rate.....	55
4.10.1 Variation between different Flow rate and Temperature Different.....	55
4.10.2 Variation between different Flow rate and Thermal Resistant.....	56
4.10.3 Variation between different Flow rate and Heat Transfer Coefficient....	57
4.10.4 Variation between different Flow rate and Nusselt number.....	58
4.10.5 Variation between different Flow rate and Pressure Drop	59
4.10.6 Variation between different Flow rate and Pumping Power	60
CHAPTER 5: CONCLUSION AND RECOMMENDATION	61
5.1 Conclusions	61
5.2 Recommendation for future works	63

References	64
Appendix	69

University of Malaya

LIST OF FIGURES

Figure 2.1: SIMPLE Method flow chart	23
Figure 3.1: Flowchart of research methodology.	25
Figure 3.2: Picture of MCHS test piece (autodesk.com)	26
Figure 3.3: Details view of microchannel heat sink.....	26
Figure 3.4: Microchannel heat sink (Schematic view).....	27
Figure 3.5: Structured mesh of the straight MCHS.....	28
Figure 3.6: (a) laminar hydrodynamic boundary layer development in MCHS in the constant inlet flow velocity. (b) Thermal boundary layer in MCHS with constant heat flux. (Raja Kuppusamy, 2016)	32
Figure 3.7: Computational domain of MCHS with Single Channel.	36
Figure 4.1: The temperature contours of coolant along the straight channel.....	39
Figure 4.2: Temperature different and length of straight channel	39
Figure 4.3: The temperature contours of coolant at entrance region of straight channel	41
Figure 4.4: The pressure contours of coolant along the straight channel.....	41
Figure 4.5: Velocity vector of coolant along the straight channel	42
Figure 4.6: Computational grid of numerical model MCHS	43
Figure 4.7: Model validation with prior analytical (Steinke, Mark E. Kandlikar, 2005) and numerical results (Sohel et al., 2014) Reynold number and friction factor.	44
Figure 4.8: Model validation with prior analytical (Phillips, 1988) and numerical results (Sohel et al., 2014) local Nusselt number and Dimensionless thermal length.....	45
Figure 4.9: Validation of (a) Poiseuille number (b) Pressure drop and Reynold number (Sohel ,Steinke & Kandlikar).....	48
Figure 4.10: Temperature different of the microchannel for the different aspect ratio of the channel.	49
Figure 4.11: Total and spreading thermal resistance for the different aspect ratio of the channel.	50

Figure 4.12: Heat transfer coefficient of the microchannel for the different aspect ratio of the channel.	51
Figure 4.13: Fully developed average Nusselt number and different aspect ratios of the channel	52
Figure 4.14: Relationship pressure drops of the microchannel for the different aspect ratio of the channel.....	53
Figure 4.15: Relationship pumping power of the microchannel for the different aspect ratio of the channel.....	54
Figure 4.16: Temperature Different of the microchannel for the different flow rate of the channel.	55
Figure 4.17: Thermal resistant of the microchannel for the different flow rate of the channel.	56
Figure 4.18: Heat transfer coefficient of the microchannel for the different flow rate of the channel.	57
Figure 4.19: Fully developed Nusselt number and different flow rate	58
Figure 4.20: Pressure Drop of the microchannel for the different flow rate of the channel.	59
Figure 4.21: Pumping power of the microchannel for the different flow rate of the channel.	60

LIST OF TABLES

Table 3.1: Thermophysical properties of cooling fluid in MCHS	27
Table 3.2: Dimension of the Straight microchannel heat sink	28
Table 4.1: Present parameter data	38

University of Malaya

LIST OF SYMBOLS AND ABBREVIATIONS

A	:	solid-fluid interface area
c_p	:	heat capacity (J/kg·K)
D_c	:	hydraulic Diameter (μm)
G	:	volume flow rate (m^3/s)
h	:	heat transfer coefficient ($\text{W}/\text{m}^2\cdot\text{K}$)
H	:	height of micro channel heat sink (mm)
k	:	thermal conductivity ($\text{W}/\text{m}\cdot\text{K}$)
L	:	length of micro channel heat sink (mm)
\dot{m}	:	mass flow rate (kg/s)
MCHS	:	micro channel heat sink
n	:	local coordinate normal to the wall
Nu	:	Nusselt Number
Nu_r	:	Nusselt Number ratio
ΔP	:	pressure drop (Pa)
q	:	heat flux (W/m^2)
T	:	temperature (K)
u, v, w	:	velocity components (m/s)
T	:	temperature (K)
W_c	:	width of the channel in micro channel heat sink (mm)
W	:	total width of micro channel heat sink (mm)
x, y, z	:	Cartesian coordinates
Greek Symbols		
ρ	:	density (kg/m^3)
μ	:	viscosity ($\text{Pa}\cdot\text{s}$)

τ : wall shear stress (N)

Subscripts

f : fluid

in : inlet

out : outlet

s : solid

University of Malaya

LIST OF APPENDICES

Appendix A: Validation analytical and numerical data (Kandlikar and present study)	69
Appendix B: Validation analytical and numerical data (Philip and present study)	70
Appendix B: Validation analytical and numerical data (Philip and present study)- (Continue)	71
Appendix B: Validation analytical and numerical data (Philip and present study)- (Continue)	72
Appendix B: Validation analytical and numerical data (Philip and present study)- (Continue)	73
Appendix B: Validation analytical and numerical data (Philip and present study)- (Continue)	74
Appendix C: Validation analytical and numerical analysis (Pressure drop with Reynold number).	75
Appendix D: Validation data (Experimental and numerical analysis) obtained by Sohel, Steinke and present numerical study	76
Appendix E: Numerical result for aspect ratio and flow rate	77
Appendix E: Numerical result for aspect ratio and flow rate (Continue)	78
Appendix E: Numerical result for aspect ratio and flow rate (Continue)	79
Appendix E: Numerical result for aspect ratio and flow rate (Continue)	80
Appendix E: Numerical result for aspect ratio and flow rate (Continue)	81
Appendix F: Catalogue Heat Sink	82
Appendix F: Catalogue Heat Sink (Continue)	83
Appendix F: Catalogue Heat Sink (Continue)	84
Appendix F: Catalogue Heat Sink (Continue)	85

Appendix F: Catalogue Heat Sink (Continue)	86
Appendix F: Catalogue Heat Sink (Continue)	87
Appendix F: Catalogue Heat Sink (Continue)	88
Appendix F: Catalogue Heat Sink (Continue)	89
Appendix F: Catalogue Heat Sink (Continue)	90
Appendix F: Catalogue Heat Sink (Continue)	91

University of Malaya

CHAPTER 1: INTRODUCTION

1.1 Background

Technology involving high speeds of data processing in microprocessors of fast computers has led to a reduction in sizes of integrated chips. The need to remove a large amount of heat generated from such devices for effective functional characteristics was first investigated by (Tuckerman & Pease, 1981). In their work, they had studied the experimental and theoretical performance of microchannels as heat exchangers using water as the coolant and suggested the use of high aspect ratio microchannels to reduce thermal resistance.

Semiconductor device technologies development since the middle of twentieth century leads to miniaturization of many sensors and components into microelectromechanical devices. The amount of heat flux produces by these devices increase exponentially due to the downsizing and their increasing in functionality. These amounts of heat from such small volume or surface area cannot be efficiently dissipated using conventional cooling method. Microchannel heat sinks (MCHS) proved to remove heat faster than conventional heat sink devices by their massive heat transfer surface-to-volume ratio (Sobhan, Choondal B and Garimella, 2001). Therefore, MCHS can be a good candidate in the selection of advanced cooling methods which capable to dissipate heat from tiny surface area with higher heat fluxes (Bayazitoglu, 2011) and (Zhang, HY and Pinjala, et al, 2005).

According to Moore' Law, the numbers of transistors in a processor doubles up every 2.5 years and will subsequently increase its heat dissipation. Very near in future, the heat generation in CPUs will increase up to 106 W/m^2 . It has to also be noted that the CPU needs to be maintained at a temperature lower than 80°C so that it will function properly and the life expectancy will be longer. Considering the necessity of

transporting a large heat flux from miniature electronic chips, many efforts and research had been made to increase the cooling capability of the MCHS. Several thoughts were proposed with the aid of researchers to enhance the MCHS performance together with optimizing the geometry of it and running fluid.

The main objective of this research is to validate the heat transfer and flow characteristic of MCHS by using numerical analysis. Numerical simulations are executed to determine the influence of geometric parameters on the heat transfer and flow characteristic of rectangular shaped MCHS. The validation process on the numerical analysis has been carried out which the similar physical model used by (Sohel et al., 2013) was implemented. In this dimension of a physical model, the height, width, and length of the heat sink will be represented as H , W , and L respectively and H_c and W_c stand for the height and width of channels respectively. W_w refers to the width of the sidewall, while H_{top} and H_b refer to the thickness of the top plate and heat sink substrate respectively.

1.2 Problem Statement

Even though Microchannel heat sinks (MCHS) have been defined to dissipate heat at a higher rate than the conventional devices due to having a large heat transfer surface to volume ratio but this information is insufficient to implement the MCHS with passive enhancement in the practical application due to lack of study by the researcher to compare the analysis data between simulation and experimental approached.

Despite a lot of numerical and analytical analyses had been accomplished on cooling systems for electronics machine in the published journal, the number of experimental studies carried out may be very confined to the high-quality of the author's expertise. This becomes the core inspiration behind this experimental examine, to be able to be very helpful in getting better a few research hole on microchannel heat sink.

1.3 Scope of Study

This research is mainly focused on the validation of thermal enhancement in the microchannel heat sink (MCHS) and its effect on the thermal and flow performance by using numerical analysis approach.

1.4 Objective of Study

The objectives of this study can be outlined as the followings:

- Validate the thermal enhancement parameter in microchannel heat sink MCHS through analytical and numerical method.
- Study on the characteristics of heat transfer and fluid flow of pure water in MCHS and effect of the flow rate and aspect ratios are varied.

1.5 Methodology

This research began with the extensive revision on previous published literature evaluations to achieve a better understanding of the verification methods to be had, mainly for the microchannel heat sink MCHS. A number of sources covers include the scholarly journal, book, conference paper which related to the field of study are reviewed. The purpose of literature review was used to establish a theoretical framework and validate the initial consequences of the existing studies. The numerical model is obtained through previous research and literature which after that proved with the available results outcomes. It is then analyzed based on the aims of this research study. The data attained from the research were accumulated, analyzed, interpreted and then expressed in graphical and tabulation form for better understanding.

1.5.1 Model benchmark and analysis.

Model and Analysis

The heat sink has various types, shapes and sizes depend on the application. Microchannel heat sinks (MCHS) has been chosen for this study because of it is proven having a higher rate of heat dissipation than the conventional devices. The design and size of the microchannel will be based on the standard MCHS model (Steinke & Kandlikar, 2006) and (Sohel et al., 2014) selected as a benchmark model.

Remodeling

The next step of this project is to remodel the part. To generate a 3D design, software of SOLID WORKS was used. All the design will be attached to this report to view and analysis purpose. The CAD design was drawn by solid work software and will be imported to the CFD software for details result simulation.

CFD analysis

A numerical model is turned into formulation to solve the three-dimensional heat transfer in microchannel heat sink using the commercial CFD software package, FLUENT. The simulation can be acting on one set of dimensions. The design and size of the microchannel will be will be based on the standard MCHS model. The model might be run through a series of meshing refinement to raise the accuracy of the analysis. Then a full-scale analysis will be conducted to validate the flow and heat transfer characteristic of the microchannel. The Reynold number and the Nusselt number will be evaluated.

1.5.2 Validation

Validation for both analytical and simulation analysis on the flow and heat transfer characteristic onto the profile of the MCHS will be compared and to justify future improvement and enhancement analysis. The numerical model was developed by referring to the previous published works of literature which after that proved by the available results outcomes and correlations. The model is then studied based on the aims of this research.

The data attained from the experiment is gathered, analyzed, interpreted and presented in graphical and tabulation method for clearer understanding. Last but not least, the overall flow of this research study begins with the literature reviews, research methodology, results and discussion, and followed by the conclusion were attached into a research thesis.

1.6 Outline of the Thesis

This thesis comprises a total of five chapters. The arrangement as the following:

Chapter 1, Explain the background, problem statement, objectives, scope of the study and the methodology of the research or studies.

Chapter 2, provides previous studies or research develop from various sources which relevant and similar to the research topic to support the topic.

Chapter 3, explain the method and principles applied included the grid independent test, governing equation and its solving technique in Computational Fluid Dynamics (CFD) that has been applied during this investigation.

Chapter 4, presentation of the results output of the analysis and discussion on the results with relevant chart or table attached.

Chapter 5, discussion and conclusion obtained from the research.

University of Malaya

CHAPTER 2: LITERATURE REVIEW

2.1 Introduction

Today, world have to be in a present where electronic segment to a great extent, utilized as a part of our day by day life. Due to rapid increase in heat dissipation of electronic devices, super cooling technology is needed to help these electronic devices to work efficiently. MCHS is one of technology that available and can increase the cooling rate. The advantages for using this component are it is compact, lighter and possess more surface area thus help in improving the heat transfer rate. Computational Fluid Dynamics (CFD) is the tools that widely used in industry to generate the thermal analyze. This software is easy to use for analyze even the geometry is complex. By using this software, the times taken to analyze the flow and heat transfer are fast and low cost. The advantages of CFD make it become popular in the market and also any researchers. It also has generated a new specialist as testing engineer of heat transfer in electronic industry. In general, the users and code developers are trying to make a benchmarking and validation of CFD. Before this, the studies of micro channel flows are the various topics. There are many researchers that already make the experiment on the effect of heat transfer and friction factor in micro channels heat sink. On every research, the main point of this topic is cooling configuration.

2.2 Microchannel Concepts

In the earlier stage, the MCHS was discovered by (Tuckerman & Pease, 1981) in early 1980's. They used silicon as material and also used water as cooler liquid. It is used to dissipate the heat from an electronic chip. The dimension of silicon MCHS is 1 cm². They stated that, the diameter of width of the channel will affect the thermal boundary layer thickness. The resistance of convective will be reduces when the thickness decrease, thus increase the cooling rate. (Wu & Little, 1984) run an experiment about fluid flow in MCHS for gas flow. As a result, they realized that in

laminar regime has higher friction factor compare to turbulent. The Reynolds number around 350 to 900. (X. Wang, 1994) also run the experiments on MCHS. He got the changes of laminar to turbulent state occur at Reynold numbers are lower than what he expected as a theory. Besides that, (Peng & Peterson, 1995) found a small different between results of theoretically and experimental. They run the experiment of MCHS of 133 μm to 367 μm hydraulic diameter and the results come out with the friction factor is dependence on hydraulic diameter and size of channels. (Judy, Cheng, yal et al, 2002) run an experiment of pressure drop on square and round of MCHS. The hydraulic diameter of the channel for this experiment is around 15 to 150 μm . They used different liquid cooler like distilled water, methanol and isopropanol in range of 8 to 2300 Reynolds number. The results show no different between the liquid coolers when tested with laminar flow. (Liu, Dong and Garimella, 2004) run an experiment of pressure drop and visualization on hydraulic diameter around 244 to 974 μm with combination Reynolds number in range 230 to 6500. They made the comparison between pressure drop and numerical calculations. They also used computational method to get the overall averaged Nu number and Re number on different pressure drops in MCHS. (Choi, SB et al, 1991) referred to their experiments and continue with MCHS in diameter 3 to 81 μm . They assume the Nusselt number depends on Reynolds number. The experimental of heat transfer and pressure drop also made by (Muhammad M Rahman & Gui, 1993). He tested the MCHS with different depths by using water as liquid cooler.

Nowadays, the technology of electronic increases rapidly thus the manufacturers trying to increase the speed, more powerful and safe. As a result, the cooling system also must be efficient to dissipate the heat. Actually this phenomenon can be observed in our daily life. Basically the computer chips are cooled by air fan but when this computer needs to run in high frequencies, it will create large amount of heat. Thus, the

standard cooling methods are not compatible with the system. Therefore, they analyze are still in running to produce a powerful method to dissipate the heat.

The first thing that needs to understand is the concept of water convection by learning the heat transfer and concepts of energy. The meaning of heat transfer is the energy transit because of the change of temperature. Conduction, convection and radiation are the three main concept of heat transfer. The most useful in this experiment is convection. This is because the heat transfer occurs between solid surface and moving water or any liquids. The convection happens when there is different temperature between solid and moving liquids.

2.3 Analytical Studies

In 1980s, (Tuckerman, 1984) focused on flow friction and heat transfers that affect microchannel heat sink. He already does his study on different dimensions. After that he developed certain parameter of the channel that can produce high heat transfer. He made a conclusion that the study of heat transfers in the microchannel can be done by focused on the flow through them like single-phase flow or two-phase flow. Therefore, the next generation will focus on this two type phase for further study.

In 1998, (Poh & Ng, 1998) continued the study on single phase liquid flow. They used ANSYS software to analysis the phenomena that happen on microchannel heat sinks. They already used sixteen different situations on different height, width, length, wall heat flux and also the inlet velocity of the coolant. On the study they maintain the properties of fluid and velocity of inlet, laminar flow, constant the heat flux, no pressure and velocity gradients at the end of the heat sink. Based on their analysis the thermal resistance will increased when they made the adjustment of microchannel by decrease the depth, increase the width and decrease the inlet velocity.

Besides that, (Zeighami et al., 2000) focused on the behavior changes of water as their coolant in heat sink flow laminar to turbulent. Before this, researches already discovered that the transition of the flow happened when Reynolds number is lower than 2200. Basically it occurs because of the effect of the surface roughness and viscous heating. Furthermore, the transition Reynold number of microscopic level still cannot be calculated by using analytically except by experimental.

(Muhammad Mustafizur Rahman, 2000) studied the heat transfer and the pressure drop of different shape on microchannel heat sinks. There were I-channels and U-channels. The fluid flows of them were totally different from each other. The width of the channel was 1 mm and depth was around 176 to 278 μm . The coolant for his study is water. Therefore, he observed the changes on temperature and pressure of the water around the channel. He discovers that the Nusselt number will be higher at the inlet.

(Zhi-Xin Li, 2003) focused on the surface roughness of the microchannel heat sink. After that, he observed the changes of Reynold number when used different roughness. They used stainless steel as the material of the microchannel with different diameters like 128.8, 136.5 and 179.8 μm . The value of surface roughness of the materials was on the range from 0.03 to 0.043. From their analysis, the theory value of Reynold numbers was in the range 500 to 2000. Thus the transition Reynold numbers from laminar to turbulent flow were around 1800. He also suggested producing a passage on the fins through cutting. By doing this, the pressure drop was really increased thus improving the rate of heat transfer.

In the year of 2000, an investigation regarding the convective-conductive heat transfer was done by (David and Rector et al, 2000) due to a laminar boundary layer flow of the stream over dimensional reveal of rectangular chip squares which express to the limited heat assets. A period specific numerical plan calculation, PISO (pressure-

implicit with splitting of operators), has been applied to invigorate the conjugate heat transfer between the liquid and solid ranges. The ultimate outcomes of the recreations show the present of the variation of squares caused stream stagnant locales between pieces in which restricted the heat changed over to the encompassing stream field. By opening the chip board between square, the heat transfer of zone between pieces can be enhanced passively. The upgrade of the heat transfers consequently happening is apparently because of pseudo-suction powers with actuates a vertical stream among squares. The addition target Nusselt number on the chip pieces reflect the heat transfer for the chip-on-board, predominantly discovered further downstream of the stream course on the west sides of the chips. In additional, there was also investigation which proved that the temperature variations from chip-to-chip decrease if the openings discovered upstream of the front-end square and downstream or the backside pieces are fixed. His ideal about the variety of chip pieces cooling setup is good enough for a gadgets business.

(Li & Olsen, 2006) tried to approve the CFD package FLUENT with the trial data got by then some time recently. They have successfully carried out two investigations on the heated chip with a temperature of 353K and the air channel speed at 293K. The velocities were varying in the range from 1m/s to a maximum of 7 m/s. The effect of the heat transfer rate on the straight channel stream has been managed with concerning on both the completely created and uniform condition through various turbulence models attempts. Furthermore, in order to concern about both the completely created and uniform condition, controlling on the heat transfer rate of substrate adiabatic is necessary. The numerically chosen is alike to the heat transfer of the substrate adiabatic. The results show that the stream in the region of the module is three dimensional, and presentations stream division and vortex progression, subsequently prompting a mind boggling circulation of the neighborhood heat transfer coefficient on the substrate. At

the point when all is said in done the stream structure was in great concurrence with the examinations. The expected turbulence control did not settle well with the estimations. The turbulence treatment near the divider is fundamental and divider limits are not reasonable.

(Dhiman and A.K., and Choi, W.K., 2000) explored the stream and characteristics of heat transfer of a separated crossflow square chamber set symmetrically in a planar opening for a scope of conditions. The solid square chamber heat transfer networks were attained in crossflow. Furthermore, the blockage allocates on drag coefficient and heat transfer and the part of Prandtl number was clarified by the Nusselt number variations on each face of the obstruction and agent isotherm.

(Judy, Maynes, & Webb, 2002) numerically investigated the liquid stream and heat transfer traits of mixed convection with four heat sources in three-dimensional rectangular channel. Four parameters were measured on their effect including transport, heat source, channel build, Richardson number and gradient point. The SIMPLE count was associated with control coupling in central of velocity and pressure, and new high-arrange safety guaranteed second-arrange difference plan was established to discretize the convection term. The advanced convective heat transfer is not just linked to the temperature field and velocity field, as well as the collaboration between them, analyzed by the numerical results from the point of view of the field compliant energy standard. With the field cooperative energy guideline, the effects of the parameters for the heat execution would be able to be simplified. Subsequently, the cooperative energy between the temperature and velocity slant should be extended in order to obtain the enhanced electronic cooling when diverse conditions are unaltered.

(Setal, 2004) examined the unpredictable unsteady flow around and through a channel by explaining specifically the unsteady Navier-Stokes equations in the

existence of an obstruction at the entry. They considered the Reynolds quantities of 4000, as exploratory outcomes are accessible for examination. The registered outcomes are in close concurrence through investigations. A better comprehension of the liquid pumping and the marvel of converse flow is used to support the calculations.

(Roy and Aet, 2002) directed comparative sort of examinations by adding to a completely unequivocal two-dimensional incompressible laminar Navier-Stokes solver in primitive variable definition utilizing a Cartesian stunned framework. The representing stream mathematical statements have been tackled on the physical plane utilizing a limited volume discretization plan. They discretized the convective terms of the weighted second upwind design. The sola wright correction estimation method was used to handle the mass. Next, central differencing plan is distinct by using the diffuse terms of the energy mathematical statements. Apart from that, two blockage extents, particularly, 0.125 with four different unmistakable Reynolds numbers, to be particular, 150, 300, 750 and 1500 were used to handle the stream past a square chamber set in a channel. The typical drag coefficient rises with an augmentation in blockage extent for a given Reynolds number. Distribution zones are framed on the channel divider surfaces for Reynolds number 750 and 1500, individually. Recycling zones on the dividers are influenced by the vortex peeling procedure. Their structure and area become changed every once in a while. Streamlines, vorticity shapes and weight forms are given to dissect the essential attributes of the stream field. The outcomes contrast well and those accessible from writing

.(Rodgers, 2003) evaluated the numerical prescient precision for sections printed circuit board (PCB) which heat move in constrained convection utilizing a generally utilized computational fluid dynamic (CFD) programming, such as segment intersection temperature expectation exactness for the occupied panel case is regularly inside 65°C

or 610% which would not be adequate for temperature forecasts to remain utilized as limit circumstances for ensuing dependability and electrical execution investigations. Neither the laminar or turbulent flow stream determines the entire stream fields, proposing the requirement for a turbulence stream equipped for demonstrating move. They demonstrate that the full multifaceted nature of segment thermal interface is not to be completely caught.

(Anderson, 2003) Exhibited an analytical approach for characterizing electronic packages, in view of the Laplace on the steady state condition for general rectangular geometries, where the boundary conditions are consistently indicated over particular areas of the package. A general three-dimensional Fourier is a basic arrangement that offers a means of gaining a unique analytical solution for complex IC packages which fulfills the conductions at the interfaces film, package board and fluid-liquid. A strategy was prevailed by them to regulate the intersection to-surrounding thermal resistant and count for operational conditions by rectifying the thermal resistance of electronics components. Besides that, the analytical method offers an exact and effective arrangement system for the thermal characterization of electronic bundles showed by the contrasted between the qualities and distributed experimental information for both a plastic quad flat package and a multichip module. Two factor has been projected for force convection applications which are the main records for any upstream streamlined unsettling influence and the second mentioning about purely thermal interaction. In this manner, the two components are joined if an upstream powered part interfaces with a downstream segment. They found that the two components might be qualified as far as promptly measured temperatures and after that utilized as coefficients to alter the standard thermal resistance information for operating conditions. Furthermore, this method was applied to deal with a symmetrical array of board mounted 160-lead devices. The result outcomes showed how the variables change by different part

position, Reynolds number and non-dimensional power distribution. Based on the information they suggested another strategy for creating operational segment thermal resistance.

2.4 Numerical Studies

Heat transfer wonder in small scale channel heat sinks utilizing three-dimensional numerical examination was researched by (Qu & Mudawar, 2002) and (Kohl, Abdel-Khalik, et al, 2005). This paper showed the use of water as the cooling fluid in three-dimensional fluid stream caused a poor heat transfer in a rectangular microchannel heat sink. The heat sink covers 1cm² silicon water with a width of 57 μ m and a significant of 180 μ m of scales of channel, and are separated by a 43 μ m divider. A numerical code in light of the limited contrast technique and the SIMPLE calculation is created to explain the representing mathematical statements. By examination, it is discovered that the temperature rises along the stream course in the solid and fluid zones can be approximated as direct. The most significant temperature is experienced on the heated base surface of the heat sink promptly over the channel outlet. The Nusselt number and heat flux have substantially higher qualities near the channel delta and move around the channel sideline, moving closer to zero in the corners. A completely created stream may not be accomplished inside the heat sink for a decently high Reynolds number or at 1400. The heat sink base surface temperature will be diminished by extending the thermal conductivity of the solid substrate, especially when it is close to the outlet of the channel.

(Hestsroni, R., Laser et al, 2000) and (Lee, S.Y., Wereley, et al, 2002) separated the effect of geometry on flow stream and heat transfer, finding that a relentlessly uniform heat flux transition achieved an extended variation from the norm of temperature course on the chip surface.

Examination of two-layered microchannel heat sink thought in electronic cooling was suggested by (K Kambiz, K.V., and Adrian, 2004) this effort exhibits another thought for a two-layered microchannel heat sink with counter present stream plan for the cooling electronic parts is projected. The heat expressions and temperature circulation of these sorts microchannel were broke down and an arrangement of enhancing the geometrical outline parameters is presented the stream wise temperature ascend on the heat sink surface was observed to be significantly diminished contrasted with that of the one-layered heat sink. It can be concluded that the two-layered microchannel heat sink arrangement is a significant change over the conventional one-layer microchannel heat sink. This investigation scope is on the heat protection, temperature distribution and the enhancement of geometrical framework parameters. (Li, Ewoldt, & Olsen, 2005) investigated the experimental and numerical Micro-Channel Heat sinks for cooling and also numerically intense on Electronic Devices. Familiar, a computational fluid dynamic (CFD) system was used to predict the temperature flow in a smaller scale channel of heat exchanger. Results shows from the numerical reproduction remained then contrasted with exploratory information. The test information was assembled by mirroring a solitary 0.31 mm x 10 mm cross-segment small scale channel chip that was cooled using water stream convection. By applying the voltage to an aluminum warmer, the channel chip is warmed, and temperature rises from 40°C to 120°C were watched using an infrared camera, it has been resolved that an increment in the application of a high mass flux increase single-stage convection stream. The trial demonstrated that the heat resistant is permitted of the heat flux values.

Based on the previous study, they are only focused on the flow friction, heat transfer, different geometry, transition of flow from laminar to turbulent, pressure drop and surface roughness for single phase flow of microchannel heat sinks. This can be concluding that are very little study on the secondary flow of the microchannel heat

sinks has been conducted. The present paper talked only a little about the secondary flow in alternating slanted channel. Thus, the objective of the paper is to see the performance when vary the length different of slanted passage and the behavior of the flow.

Fluid flow (FLUENT) is the most important tool that is used in this research. Therefore, basic understanding of these tools is very important. Thus the explanation of this tool will be provided. Besides that, the steady-state thermal is one of the useful tools that are used in this analysis.

2.5 Laminar and Turbulence Flow

Laminar flow occurs when the fluid only flow parallel without any disturbance between the flow. Naturally, the laminar flow is in low velocity and no cross current perpendicular. The flow is in order and no eddies. This flow is not good for convection.

Turbulence is a flow that dominated by recirculation, eddies and usually randomness. To state whether the flow is laminar or turbulence depends on the Reynolds number. The flow of turbulent is broken down into the sum of a steady component and a perturbation component. This flow has high momentum convection, which is good for heat transfer.

2.6 Reynold Number

Reynolds number, Re is a dimensionless number which gives a measure of the proportion of inertia powers to viscous forces. It can used to evaluates the relative significance of these two types of forces for certain flow conditions. Reynolds numbers often emerge when performing dimensional investigation of the fluid dynamics issue and determine the dynamics similitude between different experimental cases. In microchannel heat sink, the water is flowing through the fins. The flow is affected by

the geometrical structure of the body and also the flow parameters which is the velocity and viscosity of the fluid. This is the formula for Reynolds number:

$$Re = \frac{\rho v L}{\mu} \quad (2.1)$$

Where L is the length, v is flow velocity, ρ is the fluid density and μ is the fluid kinematic viscosity. The result of Reynolds number used to describe dissimilar flow regime like laminar or turbulent flow. Laminar flow happens at low speed ($Re < 2100$) while the turbulent flows happen at high speed ($Re > 3000$).

Reynolds number is a ratio of pressure force to viscous force and the Reynolds number is proportional to velocity. As the velocity increase, higher Reynolds number will cause the air exert more pressure force on the model. While velocity decreased, then lower Reynolds number because air stick to surface model and then induce more natural viscosity effect and increase viscous force.

2.7 Boundary Layer

A boundary layer is a thin layer around a certain object. The boundary layer happens when there are certain changes in the flow pattern. The viscous forces occur when the boundary layer distorts the surrounding of non-viscous flow.

There are many types of laminar boundary layers. It can appear with different structure and circumstances in various formed. Stokes boundary is developed when a body oscillates with the thin shear layer. At the point when a relentless limit layer appended to a level plate held in an approaching unidirectional flow, the Blarius boundary layer will be create. The Coriolis Effect about a fluid rotates and viscous forces while the Ekman layers refer to convective inertia. In heat transfer, the thermal boundary will be created.

2.8 Boundary Layer Equations

The derivation of the boundary layer equations actually is one step advance step advance in the fluid dynamics. The example of the deduction equation is governing Navier-Stokes. It can be simplified by doing magnitude analysis. Because of this, the graph of partial differential equations (PDE) become parabolic instead of the elliptical form of the full Navier-Stokes equations. By using the general purpose finite volume based CFD software package, FLUENT the governing equation along with the related boundary conditions was solved. The following is a governing equation for incompressible fluid flow:

Continuity Equation

$$\nabla \cdot (\vec{v}) = 0 \quad (2.2)$$

Momentum Equation

$$\nabla \cdot (\rho \vec{v} \vec{v}) = \nabla P + \nabla \cdot (\mu \nabla \vec{v}) \quad (2.3)$$

Energy Equations

$$\nabla \cdot (\rho \vec{v} c_p T) = \nabla \cdot (k \nabla T) \text{ (Liquid)} \quad (2.4)$$

$$\nabla \cdot (k \nabla T) = 0 \text{ (Solid)} \quad (2.5)$$

2.9 Computational Fluid Dynamics (CFD)

Computational means doing with mathematics, computing and fluid dynamics means the dynamics behavior in fluid flow stream. With using CFD, a computational model can be constructed to represent a system or device that we want to study. At that point fluid flow physic and chemistry will be applied to the 3D model, and the software will solve the governing equation on order to predict the dynamics of fluid flow inside the boundary region with physical phenomena such as vortex, natural heat convection, etc. CFD is a refined computationally-based design and analyze technique. CFD programming provides multiphase physics, chemical reaction, fluid-structure, heat and mass transfer, moving bodies, modelling. Utilizing CFD programming, a prototype that

resembles the system or device virtually can be developed to study and analyze the real-world physics and chemistry applied to the model. Then, the CFD post processing module will visualize the result and data into images (i.e. pressure contour, stream line, velocity vector, etc.) and graph plots. that predicts the performance of physical prototype.

The SOLIDWORKS is used to create a 3D model. Therefore, this model is imported to CFD for analysis purpose. Every point of model will have a set of certain governing equations for analysis purpose. The governing equations are consist of thermodynamic laws such as energy, mass and momentum. The equations also implement certain physical laws of them. Basically the energy cannot be creating or destroyed but it still can be transfer from one form to another.

The best technique to solve simple linear problems through discretization is by using numerically than analytically method. However, by using this method special care are needed to be done to make sure the discontinuous solutions can be handling gracefully. The Euler and Navier-Stokes equations are used to handle this method.

Besides that, certain discretization method is also used like Finite Volume Method. It is a volume method that generally used in commercial software. The discrete control volumes are used to explain the governing equations.

$$\frac{d}{dt} \iiint Q dV + \iint F dA = 0 \quad (2.7)$$

Here, Q represents the conserved variables vector, and F is referred to the flux vector.

2.10 FLUENT Overview

FLUENT CFD is utilized to tackle the administering basic comparisons. The preservation of mass and force utilizing administering necessary mathematical statements while vitality and other scalars such turbulence utilizing a control volume based method that comprises of:

- Used a computational framework to isolate the space into discrete control volume.
- The arithmetical comparisons for discrete ward variables like speeds, weight, temperature, and preserved scalars are built by utilizing the reconciliation of the representing mathematical statements on the individual control volumes.
- Linearization of the discretized scientific articulations and arrangement of the resultant straight evaluation structure or framework to yield advanced estimations of the subordinate variables.

2.11 Navier-Stokes Equations

These equations depend on the pressure, momentum and viscous forces in three-dimensional spaces. It is one of the fluid motion equations that usually used to perform computational fluid dynamics. Progression comparison depicts the harmony between the amounts that streaming through particular space. On the other hand, vitality comparison talks about the trade between distinctive types of vitality like potential, kinetic and heat.

The Navier-Stokes equation is actually a combination of many equations that related to the motion of fluid substances like liquid and gases. It totally depends on the differential equations to describe the motion of the fluid. However, these equations did not compulsory have the relationship with the velocity and pressure but it just only

establishing the relation rates of change. Equations below show the Navier-Stokes equations for an element in a 2D Cartesian coordinate system.

$$\begin{aligned}
 & p \left(\frac{du_x}{dt} + u_x \frac{du_x}{dx} + u_y \frac{du_x}{dy} \right) \\
 &= - \frac{dp}{dx} + \mu \left(\frac{d^2u_x}{dx^2} + \frac{d^2u_x}{dy^2} \right) + pg_x
 \end{aligned}
 \tag{2.8}$$

$$\begin{aligned}
 & p \left(\frac{du_y}{dt} + u_x \frac{du_y}{dx} + u_y \frac{du_y}{dy} \right) \\
 &= - \frac{dp}{dy} + \mu \left(\frac{d^2u_y}{dx^2} + \frac{d^2u_y}{dy^2} \right) + pg_y
 \end{aligned}
 \tag{2.9}$$

Generally, the Navier-Stokes equation is solved by using calculus step. Practically, the simplest case that can be solved by using this equation and get their exact solution is a case where non-turbulent flow in a steady state like velocity is small (small Reynold number) and has a large viscosity of the fluid.

The advantages of using Navier-Stokes equations are can define fluid flow approximately with the small scale. It is also suitable for extensive range practical problems.

2.12 SIMPLE algorithm

SIMPLE algorithm is stands for the (Semi-Implicit Method for Pressure-Linked Equations) which responding to the velocity and pressure. A simple algorithm is used in the FLUENT for analysis. Besides that, there is a better algorithm for calculation especially when the under-relaxation increases like SIMPLEC.

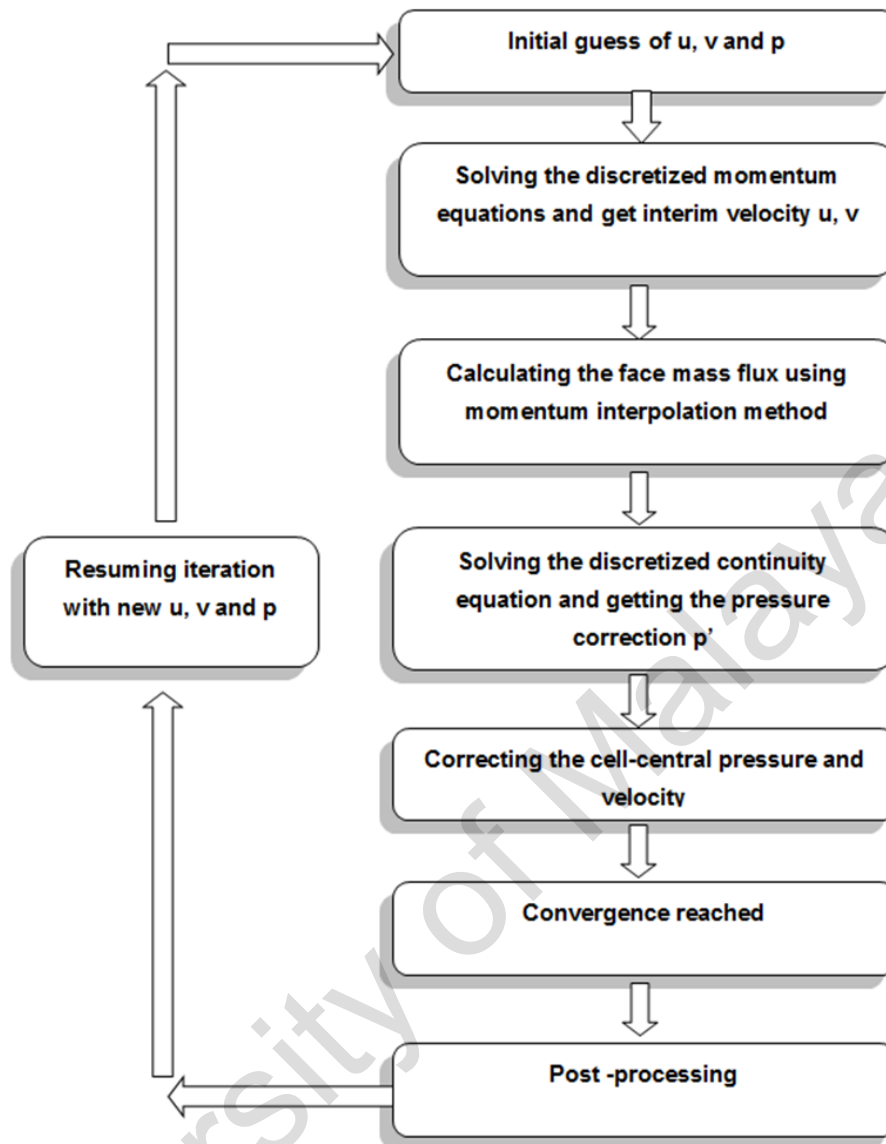


Figure 2.1: SIMPLE Method flow chart

Additionally, with using SIMPLEC, it can obtain a converged solution quicker which is an uncomplicated issue like laminar streams with no extra model actuated, where the convergence is restricted by the pressure-speed coupling. When using SIMPLEC, the pressure-correction under-relaxation factor is set to the 1.0 to make the convergence speed up. At certain problems, the use of SIMPLEC is not suitable for the solution is unstable, thus SIMPLE algorithm is chosen. Overall the flow of this SIMPLE method is visualized in Figure 2.1.

CHAPTER 3: METHODOLOGY

3.1 Outline

This section discusses the method or technique applied to analyze the flow fluid and heat transfer characteristics with passive enhancement of the MCHS. At the beginning, with conducting the literature reviews in order to understand the validation process for each experiment conducted by previous researchers. Commercial computational fluid dynamic (CFD) programming ANSYS Fluent 16.2 was used to perform the numerical analysis for this research. The reason that CFD is chosen to complete this research is that it could solve problems that associated with heat transfer which is high precision in laminar flow. CFD can efficiently simulate fluid flow in an engineering system and has contributed major savings in cost can be achieved. The computational grid together with the boundary conditions of the numerical model and computational domain are given. In addition, the thermal and flow characteristic of the mathematical foundation can be described. The preliminary result of the study is validated by using this mathematical foundation with the existing correlation. This chapter will discuss the methods of analysis, boundary condition associated and geometry configuration with referring to the previous published research and literature. Overall the flow of this project is visualized in Figure 3.1 below.

RESEARCH FLOWCHART

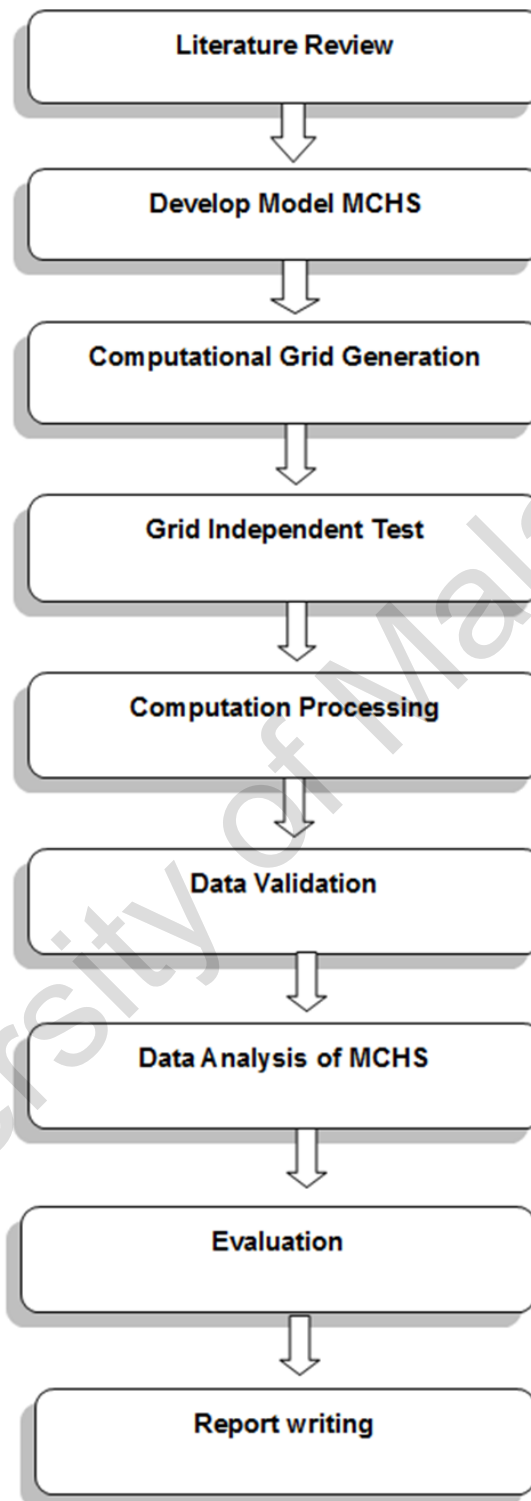


Figure 3.1: Flowchart of research methodology.

3.2 Physical Model of Microchannel heat sink

The Microchannel Heat Sink (MCHS) has an equal distance between the organized parallel straight rectangular channels (Figure 3.2). Figure 3.3 and Figure 3.4 illustrated both the details view of MCHS and schematic view respectively. The material of heat sink used normally depends on each the material's thermal conductivity. Better heat transfer rate can be achieved through higher thermal conductivity. In this project, the cooling fluid used in the microchannels of the aluminum heat sink microchannel is deionized water. Table 3.1 shows the thermophysical properties of the deionized water.

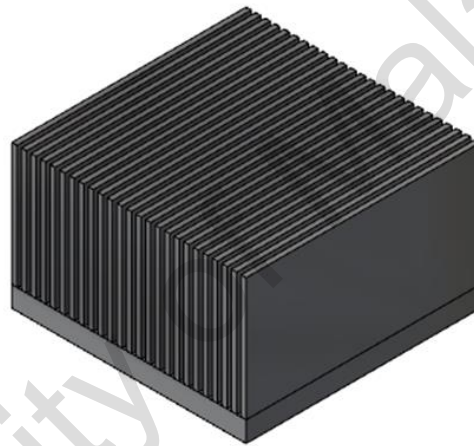


Figure 3.2: Picture of MCHS test piece (autodesk.com)

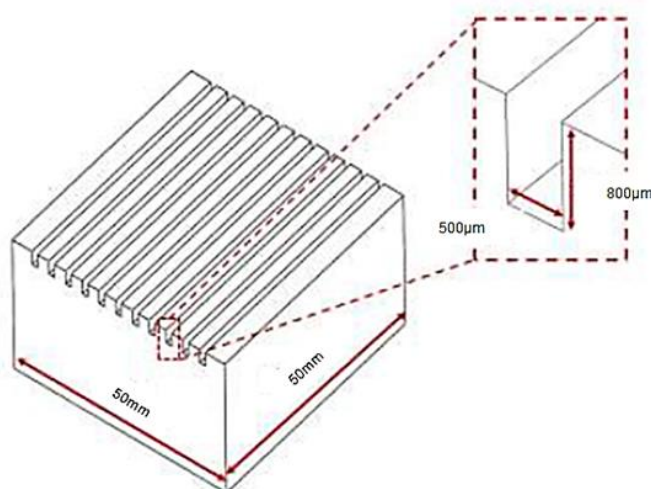


Figure 3.3: Details view of microchannel heat sink.

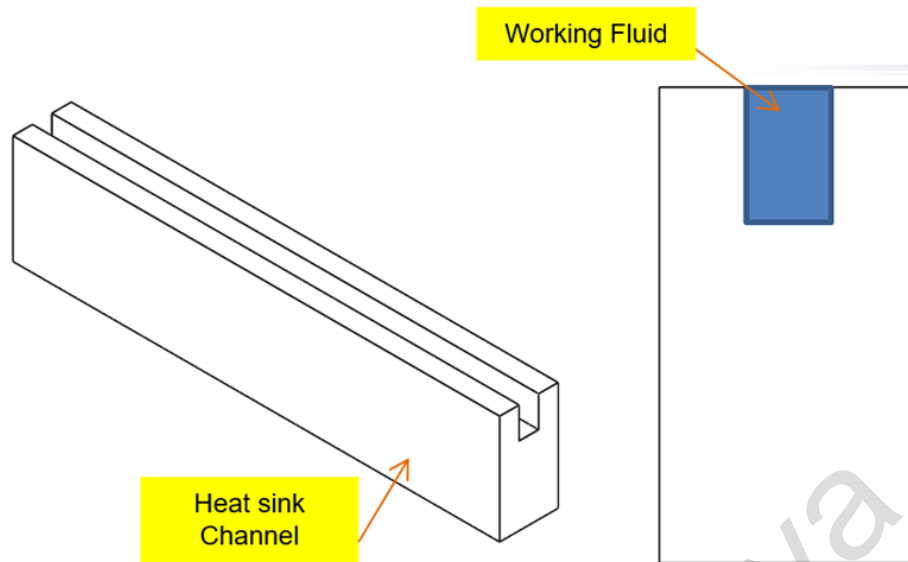


Figure 3.4: Microchannel heat sink (Schematic view).

Table 3.1: Thermophysical properties of cooling fluid in MCHS

Coolant	Density, ρ (kgm^{-3})	Thermal conductivity, K ($\text{Wm}^{-1} \text{K}^{-1}$)	Specific heat, C_p ($\text{Jkg}^{-1} \text{K}^{-1}$),
Pure water	1000	0.6	4178

Since the periodic boundary condition can be applied to each channel, a sole channel is selected from the physical model as the computational domain in order to reduce the computational time. The channel would not be considered in the computational domain because its top cover has no influence on the condition of thermal and hydrodynamic of the MCHS because it is assumed to be adiabatic. The MCHS computational domain's dimensions are based on experimental obtaining by (Sohel et al., 2014) were used and the data presented in Table 3.2.

Table 3.2: Dimension of the Straight microchannel heat sink

Channel Parameter	Values
Heat sink dimension, (mm)	50 x 50 x 10
Length of the channel, L (mm)	50
Width of the channel, W (mm)	0.5
Height of the channel, H (mm)	0.8
Number of channel	49

3.3 Computational Grid for Solution Domain of the microchannel heat sink

This section will describe briefly about the analysis of the heat transfer modeling process of the MCHS. In general, geometry creation, structure meshing and defining up of boundary conditions are comprises in the measure which solved by numerically.

Figure 3.5 below demonstrated the process in the schematic.

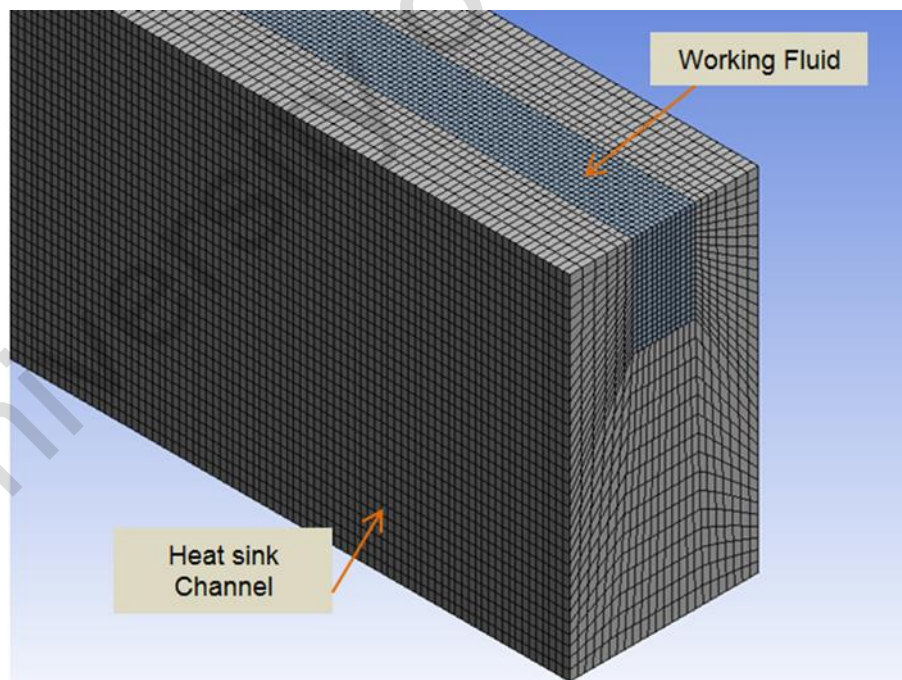


Figure 3.5: Structured mesh of the straight MCHS

3.4 Computation

The following stage involved is referred to computation and it is used Fluent 16.2, commercial CFD programming. Firstly, MCHS meshing will be load by the program and the data like a wall, wall coupled and mass flow inlet for heat transfer and pressure outlet will be given for all the boundary conditions. After that, the solution algorithms and numerical parameters will be determined. In this all-important initial condition for the evaluation is referred for the iteration process initiative. Then, Fluent will solve the energy equations, transport and conservation numerically. Furthermore, the initial guess values are used to solve the discretized forms of the equations. Finally, the achievement of convergence criteria will be succeeding when the residual of every cell in the domain reached zero.

3.5 Governing Equation

The numerical analysis based on following assumptions:

- i. The fluid flow is in steady state and incompressible condition (laminar).
- ii. The viscosity is depending on the fluid properties, except for temperature.
- iii. Gravitational force and radiation heat transfer will be neglected.
- iv. The fluid without of viscous dissipation.

There are a few equations developed based on the assumptions stated above:

3.5.1 Fluid

Continuity equation:

$$\frac{\partial}{\partial x} (\rho u) = 0 \quad (3.1)$$

Momentum equation:

$$\frac{\partial}{\partial x}(\rho_f uv) = \frac{\partial p}{\partial y} + \frac{\partial}{\partial x} \left[\mu_f \left(\frac{\partial v}{\partial x} + \frac{\partial u}{\partial y} \right) \right] \quad (3.2)$$

Energy equation:

$$\frac{\partial}{\partial x}(\rho_f u c_p T) = \frac{\partial}{\partial x} \left(k_f \frac{\partial T}{\partial x} \right) \quad (3.3)$$

3.5.2 Solid

$$\frac{\partial}{\partial x} \left(k_s \frac{\partial T}{\partial x} \right) = 0 \quad (3.4)$$

3.6 Boundary Conditions

3.6.1 Thermal Boundary Conditions

$$T_f = T_{in} = 293K$$

$$-k_f \frac{\partial T_f}{\partial x} = 0$$

at $x = 0$ (Direction 1, D1) and $x = L$

(Direction 2, D2),

at $x = L$ (Direction 1, D1) and $x = 0$

(Direction 2, D2),

No axial heat transfer in solid region.

$$-k_s \frac{\partial T_s}{\partial x} = 0$$

at $x = 0$ and $x = L$

$$\frac{\partial}{\partial y} = 0$$

at $y = 0, y = W,$

$$-k_s \frac{\partial T_s}{\partial z} = q$$

at $z = 0$

$$-k_s \frac{\partial T_s}{\partial z} = 0$$

at $z = H$

Fourier's Law defines the heat transfer conjugate between solid and fluid:

$$-k_f \left(\frac{\partial T_f}{\partial n} \right) = -k_s \left(\frac{\partial T_s}{\partial n} \right) \quad (3.5)$$

where n represents the local coordinate normal to the wall

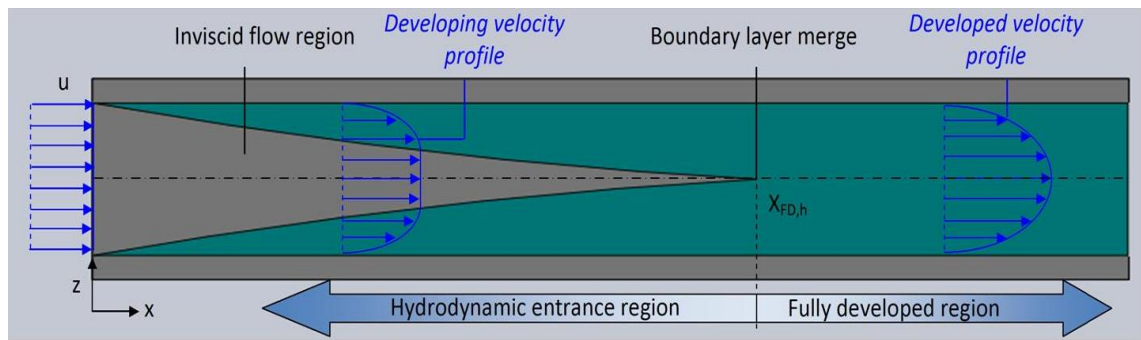
3.6.2 Hydrodynamic Boundary Conditions

$$\begin{array}{ll}
 u = v = w = 0 & \text{at the fluid-solid wall} \\
 u_f = u_{in} & \text{at } x = 0 \text{ (Direction 1, Case A) and } x \\
 & = L \text{ (Direction 2, Case B),} \\
 P_f = P_{out} = 1 \text{ atm} & \text{at } x = L \text{ (Direction 1) and } x = 0 \\
 & \text{(Direction 2),}
 \end{array}$$

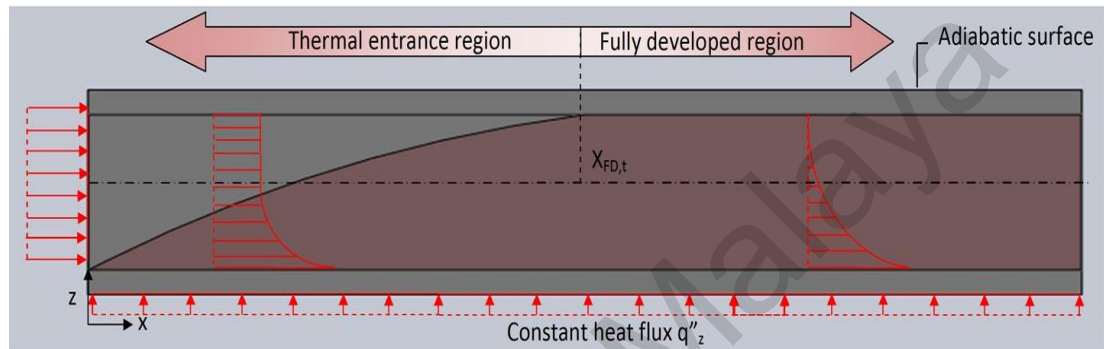
In calculating the shear stress of the wall, the fluid flow properties on both solid and fluid interface are applied. The velocity gradient at the MCHS wall for laminar flow is used to obtain the shear stress:

$$\tau_f = \mu \left(\frac{\partial u}{\partial n} \right)$$

Figure 3.2 shows a non-slip condition where the fluids enter into the wall. A boundary layer will create an inviscid core and grow throughout the channel when the fluid hits the wall at the inlet. When the boundary layers meet, the flow is considered fully developed.



(a)



(b)

Figure 3.6: (a) laminar hydrodynamic boundary layer development in MCHS in the constant inlet flow velocity. (b) Thermal boundary layer in MCHS with constant heat flux. (Raja Kuppusamy, 2016)

3.7 Solution Method

ANSYS FLUENT 16.2 in the Computational Fluid Dynamics (CFD) was used to aid in solving the equations using the finite volume based. Besides that, the second order upwind differencing scheme was used to discretize the energy and momentum convective term. Next, a SIMPLE algorithm was used to aid in solving the pressure-velocity decoupling. Except for the energy equation that is less than 10^{-8} , once the values of normalized residual reach 10^{-7} , the solutions are considered converged for all variables. In addition, both second-order upwind discretization schemes and the standard discretization are chosen for both the pressure equation, and energy and momentum equations respectively.

3.8 Mathematical Formulation

3.8.1 Thermal Characteristic

A Nusselt number represents the microchannel heat sink's thermal performance which can be calculated using equation as shown below:

$$Nu = \frac{\bar{h}D_h}{k_f} \quad (3.6)$$

where \bar{h} , $D_h = \frac{2W_c H_c}{(W_c + H_c)}$ and k_f is the average coefficient of heat convection, hydraulic diameter of the channel, and thermal conductivity of the fluid.

The equation for mean coefficient of convective heat \bar{h} :

$$\bar{h} = \frac{1}{L} \int_L h(x) \cdot dx \quad (3.7)$$

where L is the channel length.

The below equation is used to determine the coefficient of local convective heat transfer, $h(x)$:

$$h(x) = \frac{1}{\sum_{x,y} dA(x,y,z)} \left[\frac{\sum_{x,y} q''(x,y,z) dA(x,y,z)}{\sum_{xy} [T_w(x,y,z) - T_m(z)] dA(x,y,z)} \right] \quad (3.8)$$

$T_w(x,y,z)$ is the local wall temperature, and $T_m(x)$ is the local fluid bulk-mean temperature given by:

$$T_m(x) = T_{in} + \frac{1}{\dot{m}c_p} \sum_{x,y,z} q''(x,y,z) dA(x,y,z) \quad (3.9)$$

3.8.2 Fluid Characteristic

The friction factor of the fluid is calculated by using the following formula:

$$f = \frac{\Delta P D_h}{2u_m^2 \rho L} \quad (3.10)$$

where ΔP is represented pressure drop, u_m is for mean velocity, ρ is density of fluid and L is the microchannel length.

The following formula is used to calculate Reynolds number:

$$\text{Re} = \frac{\rho u_m D_h}{\mu} \quad (3.11)$$

where μ , is the viscosity of the fluid.

3.9 Finite Volume Method (FVM)

It could be very complex and tedious in resolving integral equations for the conservation of energy, momentum, and mass analytically for a 3-dimensional problem. Thus, a cheap and not costly alternative approach like CFD is necessary to solve those equations more precisely. A control-volume method is used by commercial CFD package to remedy the equations and it includes:

- A finite discrete number control volume spitted from the computational domain the use of a computational grid as shown in.
- Individual control volume including integration of the governing equations to build algebraic equations for the discrete based variables (unknowns) like conserved scalars, temperature, pressure and velocity.
- The computational node defined by grid lies in the middle of the control volume at the same time as the boundaries of the control volumes.

- The result of the resultant linear equation system and linearization of the discretized equations to yield updated values of the structured variables.

- The total of four control volume faces (six in 3D) integrals is the net flux through the control volume boundary.

3.10 Numerical method and validation

The accessible analytical equation and numerical outcomes which validated by the computational model of the conventional MCHS attaining by (Steinke, Mark E. Kandlikar, 2005), (Phillips, 1988) and (Sohel et al., 2014). Similar condition with the experiment setup carried out by Soheli et al., (2014), were applied, such as the constant heat flux from the microchannel heat sinks bottom surface, $q=1.6 \times 10^5 \text{ W/m}^2$; the velocity at the inlet cooling water, U_{in} will be varied according to the Reynolds number. Water temperature at the inlet, T_{in} , was set at 300 K in order to compare with the experimental results. The computational meshes is identified to the channel and finite volume methods (FVM) was used to solve the governing equations based on commercial FLUENT 16.2 and the SIMPLE algorithm is used to solve this conjugate heat transfer. At that point, the second-order upwind scheme had been utilized to discretize the energy and momentum equations. The solutions are said to be converged, when the governing equation on the continuity, pressure, velocity, and the residual ratio are less than 1×10^{-7} and 1×10^{-8} , respectively.

3.10.1 Analytical and numerical analysis

The validation based on mathematical equation attained by (Steinke, Mark E. Kandlikar, 2005) and (Phillips, 1988). They developed the friction factor of laminar flow in the rectangular ducts entrance region consists of two components. Firstly, is a fully develop friction factor and secondly is pressure defect known as Hagenbach factor. Besides that Steinke explained the relation of pressure drop to an apparent friction

factor. Philips has presented the Nusselt number formula with three sides heating for moderate aspect ratio channels. The derived formulation created by these researchers was used in this thesis to study in the analytical analysis.

3.10.2 Experimental analysis

To check the validity of the constructed numerical model, verification was prepared by solving the experimental model introduced by (Sohel et al., 2014) and the outcomes were compared. In this research, the geometry and working conditions are equal to those adopted in the experiments and the numerical analysis will use a single channel both sided wall. The configuration of these computational domains shows in Figure 3.7.

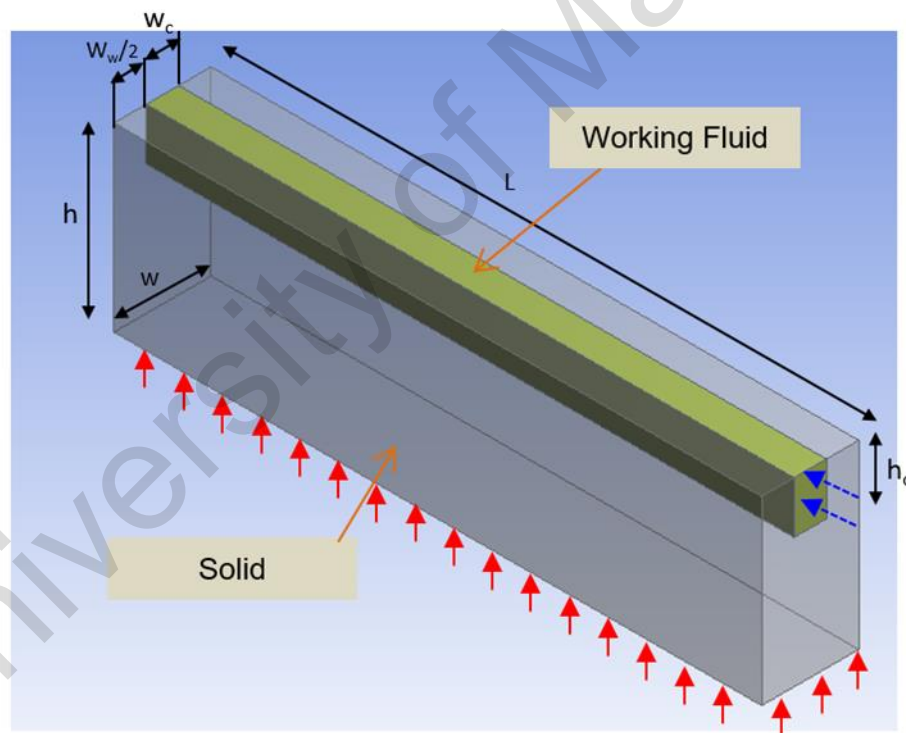


Figure 3.7: Computational domain of MCHS with Single Channel.

The experimental model carried out by (Sohel et al., 2014) is a microchannel heat sink involves rectangular microchannels with hydraulic diameter 0.6514mm, channel height 0.8mm, channel width 0.5mm and length 50mm. The numerical simulation was used to compare the data between experimental and numerical analysis. All the parameter data will be based on actual experimental with inlet velocity of 1.5m/s, an inlet temperature of 300 K and thermal boundary condition is a constant heat flux at the bottom of $1.6 \times 10^5 \text{ W/cm}^2$ and the Reynolds number ranges from 395 to 989.

A simulation with an identical boundary condition ($U_{in}=1.5\text{m/s}$, $q''=1.6 \times 10^5 \text{ W/m}^2$) and the performance of these channels will be evaluated by using solution method. The variation results for the local Reynold number, friction and pressure drop of these computational domains are studied.

University of Malaysia

CHAPTER 4: RESULTS AND DISCUSSION

4.1 Outline

The validation process of heat transfer enhancement in microchannel heat sink was carried out by comparing the analytical and numerical method and also the effect on the aspect ratio and performance of fluid flow are analyzed and interpreted in this chapter at different flow conditions. Besides that, the flow features of the working fluid and its influence on the heat transfer mechanism at the passive enhancement area will be discussed fully. The results obtained from (Sohel et al., 2014), (Phillips, 1988) and (Steinke, Mark E. Kandlikar, 2005) was compared in this study which the investigation is conducted by using similar operating condition. The validations are mainly focuses to identify the heat transfer characteristic of microchannel heat sink. The verification from the simple MCHS has been made in order to carry out this validation process, with the available numerical results and analytical equation. A boundary condition and identical geometry are used based on experiment data, obtained by (Sohel et al., 2014) which shows in Table 4.1 and some parameter data was set such as the inlet flow rate is $u_{in}=1.5\text{m/s}$ and heat flux is $q=1.6\times 10^5\text{ W/m}^2$. The analytical analysis has been conducted to identify the local and average heat transfer characteristics of the microchannel heat sink. After that, the discussion on the thermal conductivity of the solid and effects of flow Reynolds number.

Table 4.1: Present parameter data

Parameter	Present study
Heat sink dimension, mm	50 x 50 x 10
Channel width, mm	0.5
Channel height, mm	0.8
Channel length, mm	50
Number of the channel	49
Fluid flow rate, L/min	0.50-1.25
heat input, W	400
Fluid	Pure Water

4.2 Temperature Contour of Microchannel



Figure 4.1: The temperature contours of coolant along the straight channel

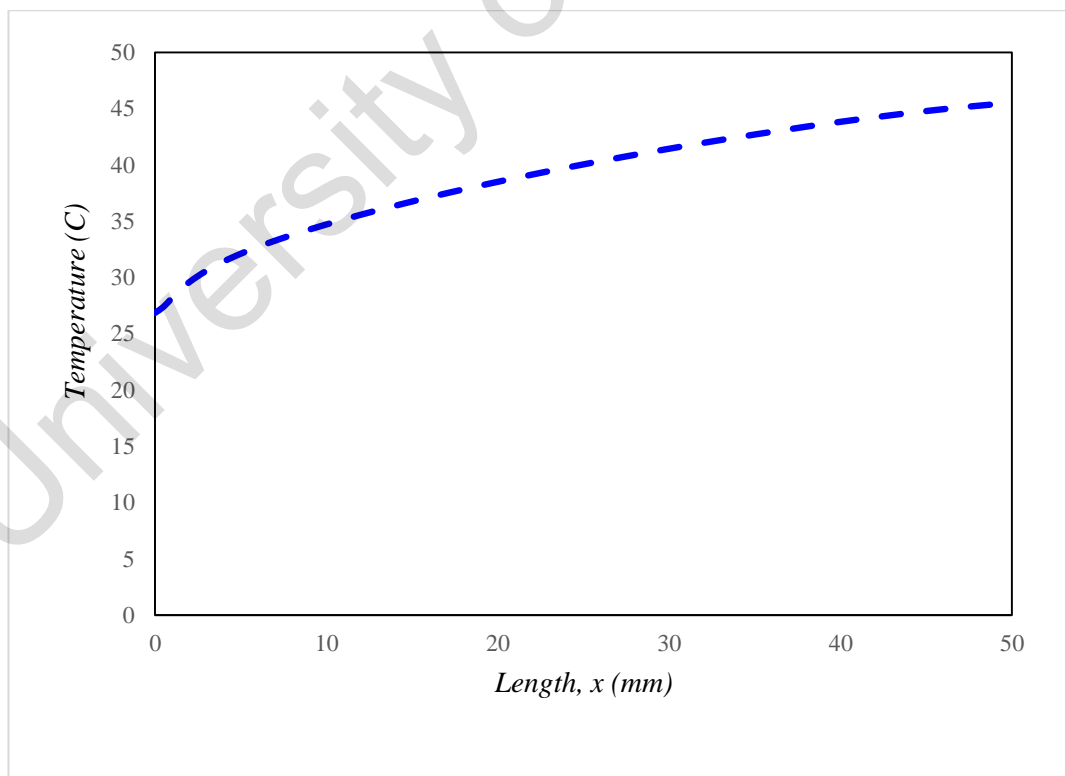


Figure 4.2: Temperature different and length of straight channel

The results obtained from the numerical analysis of the microchannel shown in Figure 4.1. The liquid flow is normally laminar and the thermal boundary layer gradually thickens. Initially, the inlet liquid temperature is uniform (at 27°C) for the straight channel. Temperature profile as shown in Figure 4.1 is the predicted hydrodynamic behavior in MCHS. It is assumed that the flow is fully developed as the heat from solid wall efficiently transferred by water. There is only thin layer of 52.63°C is existed at the solid wall. The highest temperature shown is at the channel corner. This might be due to the slow flow velocity and maximum temperature of the fluid at the channel exit.

Figure 4.2 shows the temperature variations along the channel length and it can be analyzed since the solid domain of the microchannel is directly contact with the heat source. It can be seen, the temperature increase along the flow direction of the channel and heat applied from the bottom side start increase through the solid wall and toward to the center of the channel. The temperature rises of water from 27°C to 46°C is due to solid channel walls that conducts more heat through it. Based on the results, it can be concluded that the electronics chips can dissipate heat efficiently from the aluminum material of the heat sink.

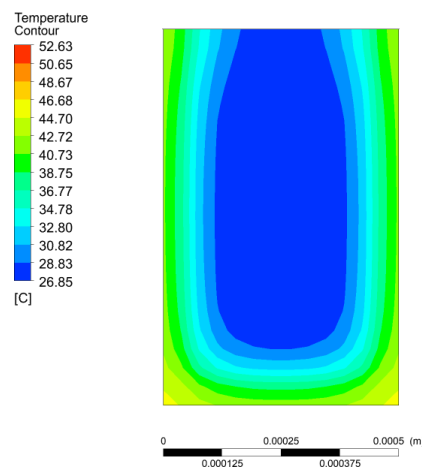


Figure 4.3: The temperature contours of coolant at entrance region of straight channel

The temperature contours at entrance region for the straight microchannel are shown in Figure 4.3. It can be observed that, the heat flux increases gradually from the bottom and both sides of the channel due to it is located nearest to heat sources and slowly moves to the center region. With the inlet velocity, 1.5m/s and heat flux $1.6 \times 10^5 \text{ W/m}^2\text{K}$, the large blue region on the center is created due to coolant starting to absorb less heat compared to the bottom and both wall channels. It can be concluded, the existing channel size or hydraulic diameter can be reduced in order to reduce the blue region area.

4.3 Pressure contour of microchannel

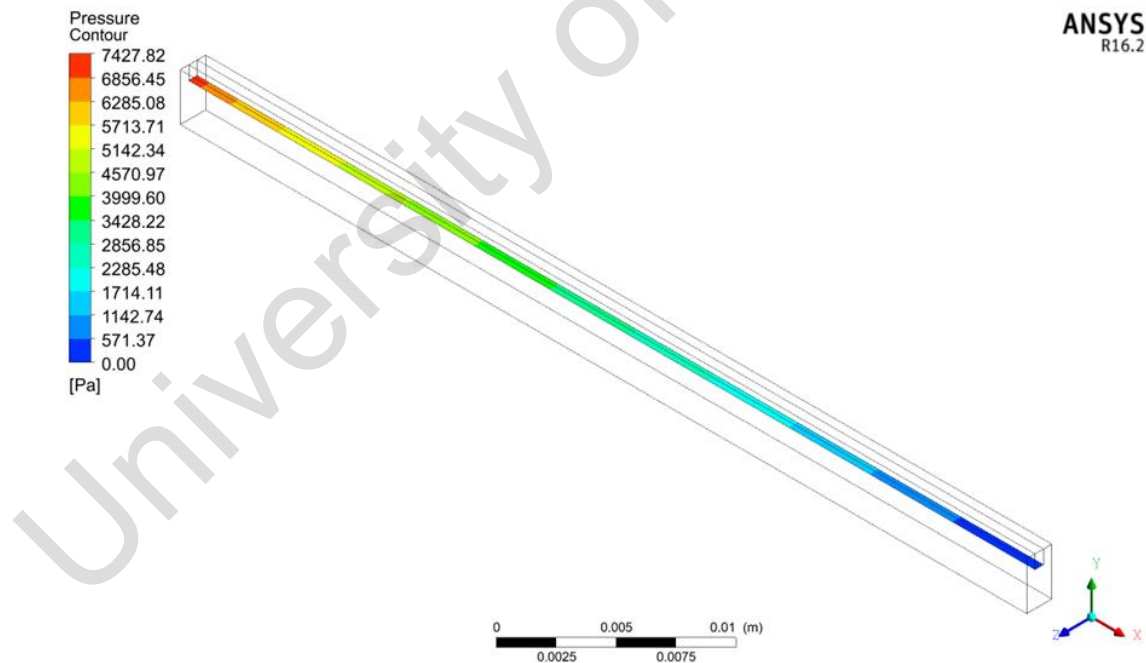


Figure 4.4: The pressure contours of coolant along the straight channel

Figure 4.4 demonstrates the pressure contours in the channel heat sink. Pressure at the inlet channel is higher at 7400 Pa and the pressure drop about 570 Pa towards the

end of the channel. Besides that, the variation of aspect ratio will also contribute to the higher of pressure drop. Pressure of liquid is going to increase as the distance increases because of heat transfer occurs between wall and liquid into the microchannel.

The current study found that with using pure water as a cooling medium is assist to get lower pressure drop due to pure water itself having lower viscosity.

4.4 Velocity Vector of microchannel

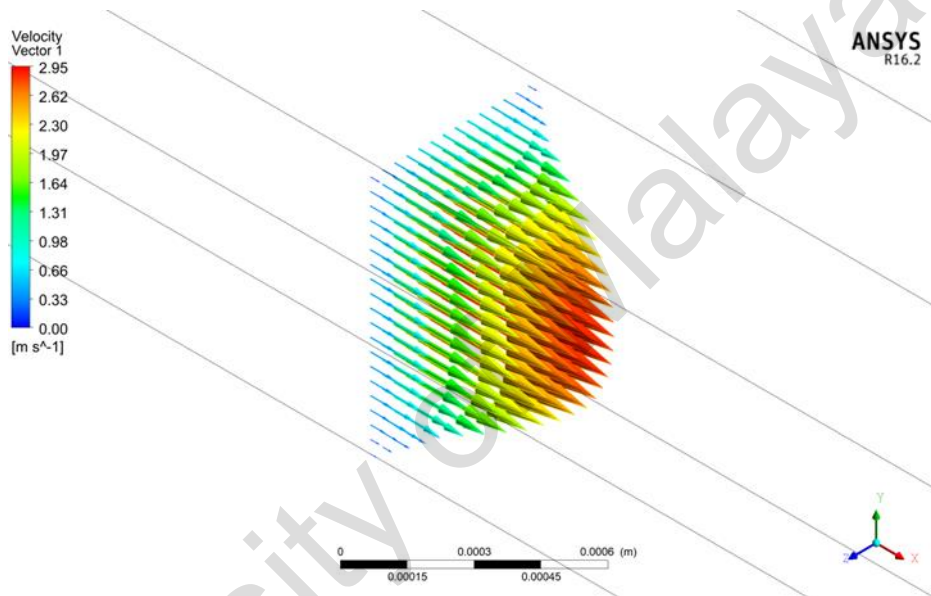


Figure 4.5: Velocity vector of coolant along the straight channel

Figure 4.5 shows the cross section of the straight microchannel at certain distance in longitudinal central (x-z) plan. It can be observed, the velocity at the center is higher around 3 m/s than the side of the solid wall, this is because of less of friction occurred and there is no resistance along the fluid flow. It can be also seen, for a straight microchannels, the velocity profile follows the parabolic distribution and the entrance region in the beginning of straight channels the flow is start developing and the velocity increased from the walls toward a center of the channel.

4.5 Grid independence study

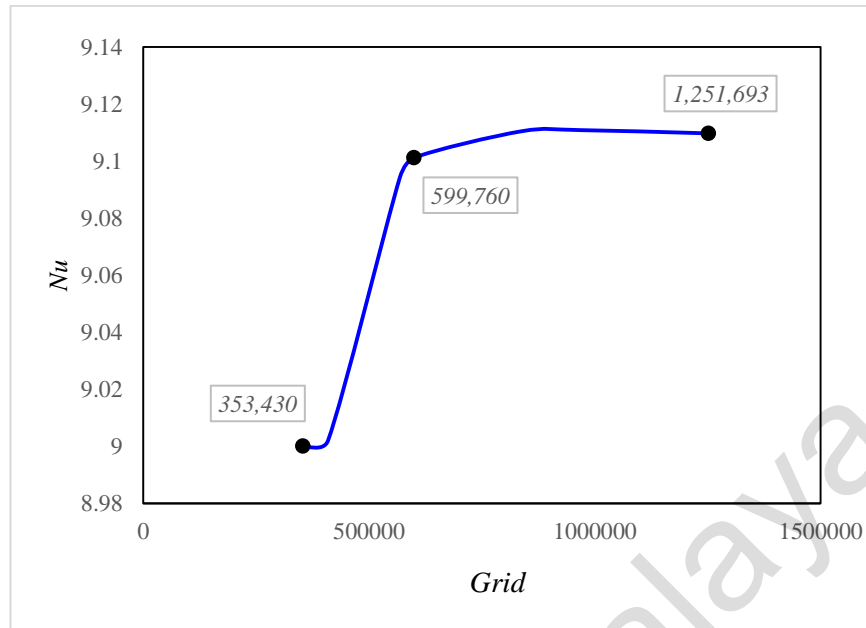


Figure 4.6: Computational grid of numerical model MCHS

The result of any numerical simulation is greatly affected by the number of elements used for discretizing the fluid and solid domains. The accuracy of the results obtained increases with increase in the number of cell elements used to discretize the domain. The type of cell elements also greatly influences the predicted results, especially in case of flow through domains such as Micro Channel Heat Sinks (MCHS).

In maintaining the accuracy of the results and at the same time reduce the computation time, the testing of the computational grid of the numerical model at different concentration in simple MCHS was shown in Figure 4.6. The coarse, fine and very fine mesh had 353,430, 599,760 and 1,251,693 nodes respectively. The less than 1% of fine mesh achieved of the percentage error was selected for further analysis.

4.6 Steinke & Kandlikar validation

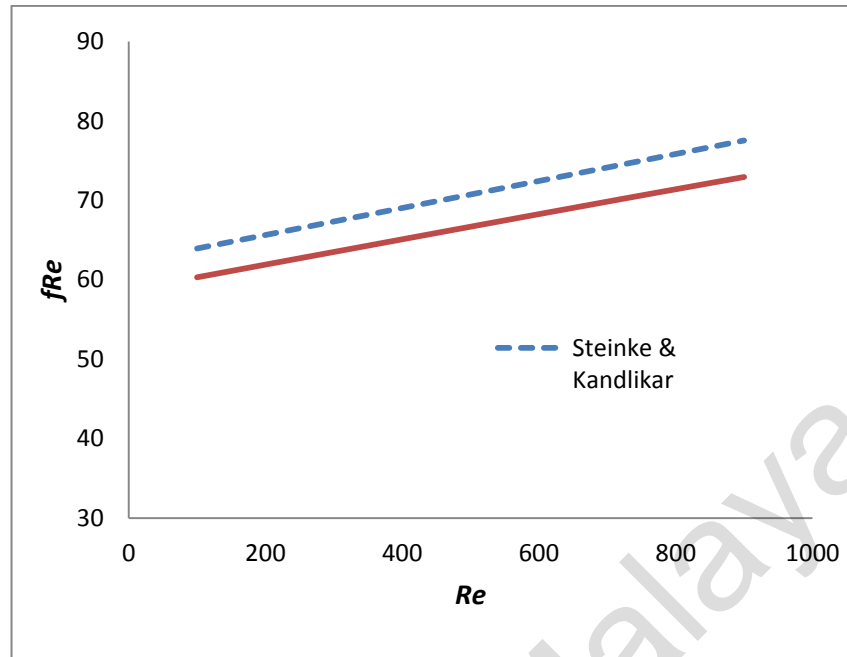


Figure 4.7: Model validation with prior analytical (Steinke, Mark E. Kandlikar, 2005) and numerical results (Sohel et al., 2014) Reynolds number and friction factor.

Figure 4.7 demonstrates the effects of friction factor and Reynolds number for the straight microchannel. A similar geometry and boundary condition are used where the inlet flow rate is $u_m = 1.5 \text{ m/s}$ and heat flux are $q = 1.6 \times 10^5 \text{ W/m}^2$. The outcome shows that the present study has a proportional graph when compare to data acquired from (Steinke, Mark E. Kandlikar, 2005), however the data is slightly lower due to the difference of the channel's hydraulic diameter (D_h) itself, where at this case the D_h size is obtained from (Sohel et al., 2014) based on 0.5 mm (W_{ch}) 0.8 mm (H_{ch}) and 50 mm (L_{ch}).

The effect on the length and hydraulic diameter of the channel size will give a lower friction factor to the present. With an increase of Reynolds number, it will increase the fluid velocity flow through the channel and heat transfer performance is significantly enhanced. Same inclination was shown by the analytical data. Thus, from Figure 4.7 there is a good covenant between the numerical and analytical data.

4.7 Philips validation

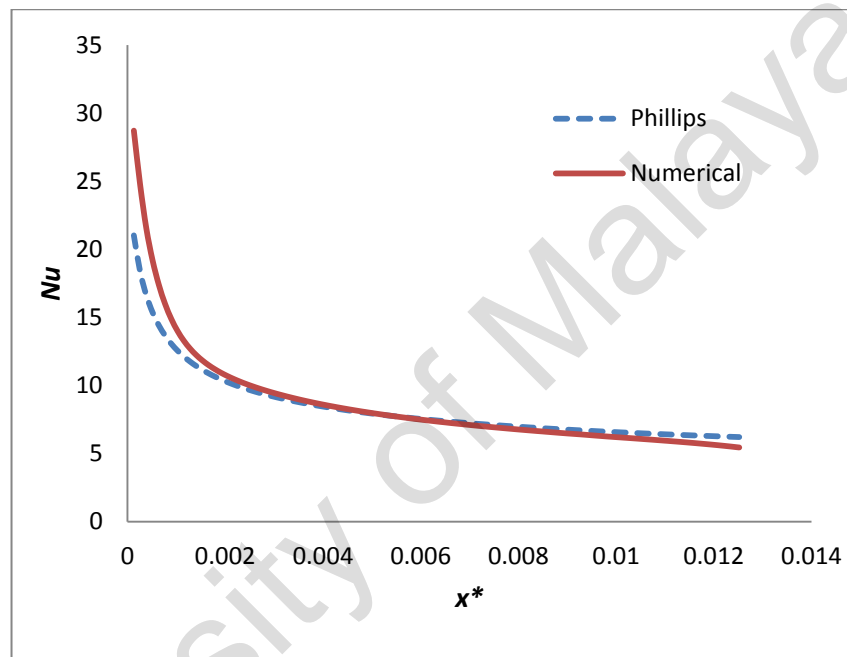


Figure 4.8: Model validation with prior analytical (Phillips, 1988) and numerical results (Sohel et al., 2014) local Nusselt number and Dimensionless thermal length

Figure 4.8 demonstrated the effect of the numerical result between a local Nusselt number and dimensionless thermal length on the microchannel heat sink. In most cases, a both sided single channel is preferable for the numerical analysis. The values calculated by the formulas for the hydrodynamically developing flow from the open literature are found to be in excellent agreement with the present numerical results. The numerical simulations for all the microchannels with different parameters of geometric

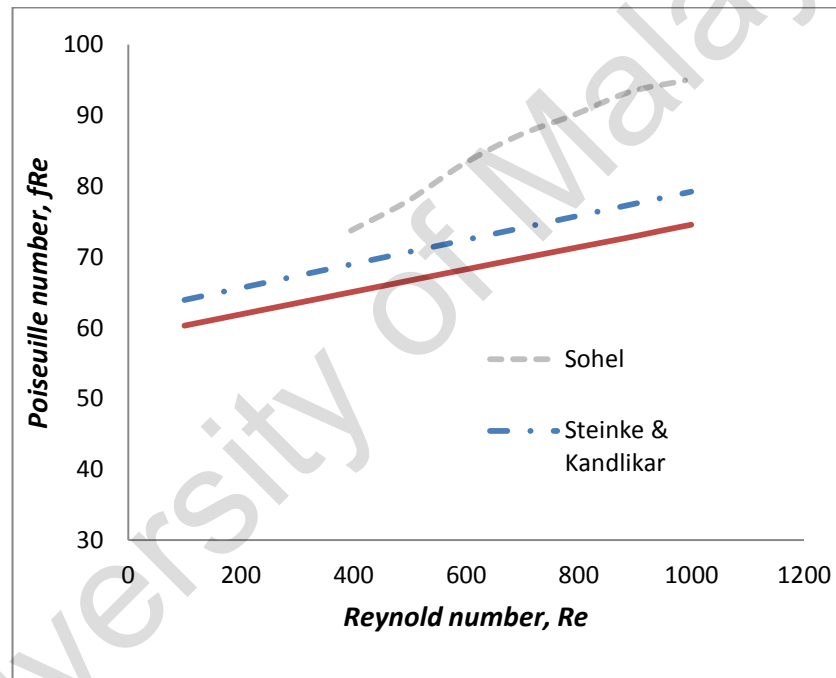
are validated from another point of view in adopting the same methods. Besides that, the maximum of mean outlet temperature for the smallest $Re = 918.68$ with $U_{in} = 1.5\text{m/s}$, $q'' = 1.6 \times 10^5 \text{ W/m}^2$ heat flux is 308.65 K , and the maximum temperature of aluminum wall is 318 K for all the numerical simulations. Hence, boiling will not be happened in this situation. A simulation with an identical boundary condition and solution method was performed to identify the variation of dimensionless thermal length and local Nusselt number. Both of these computational domains showed by the result for the local Nusselt number are comparable however the value of the Nusselt number at the beginning stage is slightly higher due to the value of initial contact surface area. An increase in initial contact surface area offers increased local convective heat transfer coefficient.

The graph also demonstrated, at the entrance of the channel, Nusselt number is starting higher and becomes smaller with downstream distance. The Nusselt number monotonically approaches a fully developed limit (assumes small property variations) if the channel is long enough. Due to this monotonic trend, the smallest Nusselt number will attain at the outlet at the channel.

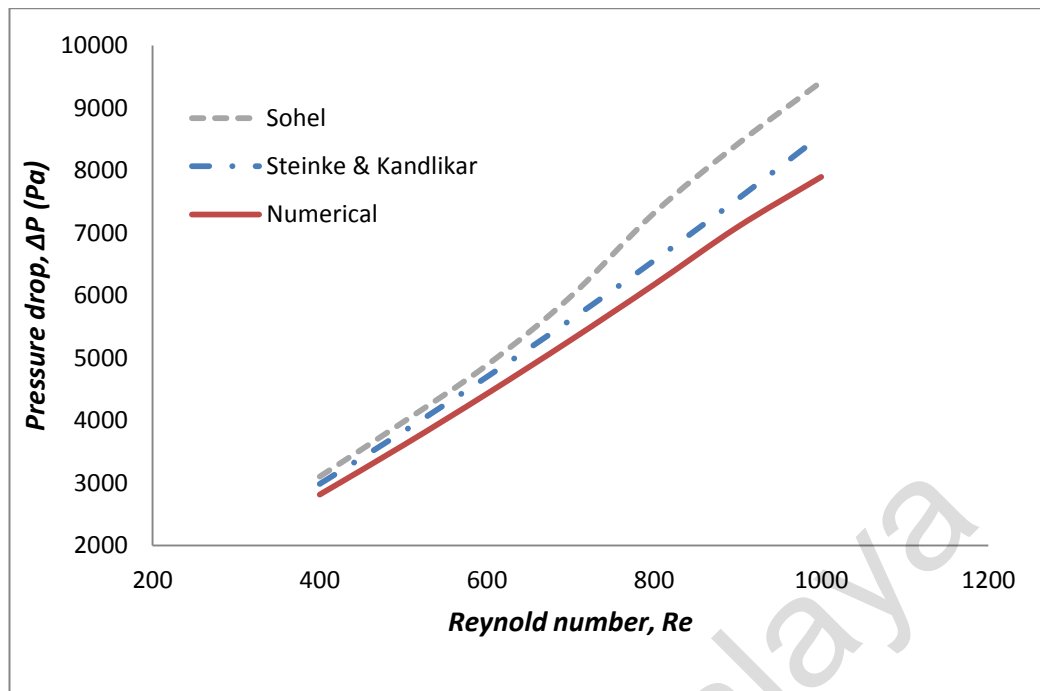
4.8 Steike & Kandlikar and Sohel

The validation process has been continued to validate from experimental data obtained by (Sohel et al., 2014) and compare with numerical results. In this experiment, the pure water and nanofluid were used as a coolant medium to absorb heat from the heat source. Figure 4.9 shows the effects of Reynold number and friction factor for the straight microchannel by comparing the experimental, numerical and analytical result. An identical boundary and geometry condition are used where the range of Reynolds number from 395 to 989 and heat flux is $q = 1.6 \times 10^5 \text{ W/m}^2$. The results show that the numerical study has a proportional graph comparing with the data obtained from

(Steinke, Mark E. Kandlikar, 2005). Based on the graph, the value of Poiseuille number, ($Po = fRe$) from experimental is higher than numerical and analytical analysis due to surface roughness and fin edges collision. Although the results showed a slightly different between experimental and numerical study, it is possible to get some idea about the better performance of the present study. With the increasing of Reynold number will increase of friction movement, therefore that the pressure drop will rise as well. So, the present study also insignificantly showed a little high friction as a consequence of the high Reynold number.



(a)



(b)

Figure 4.9: Validation of (a) Poiseuille number (b) Pressure drop and Reynold number (Sohel, Steinke & Kandlikar)

4.9 Effect of aspect ratio

The effect on the heat sink thermal performance at vary aspect ratios ($\alpha = H/W$) of the microchannel is investigated. All the input parameters (listed in Table 4.1) such as the constant value of velocity, heat flux at the footprint, length and width of microchannels. The footprint of the heat source is at a size of $50 \text{ mm} \times 1.5 \text{ mm}$. The height of the channel, H is varying to acquire various aspect ratios (α) while maintaining the channel width unchange at $150 \text{ }\mu\text{m}$. When the height of the channel increases, it offers an increased surface area for enhanced heat transfer, thus the aspect ratio also increases. With an increase in channel height, the cross-section at fluid flow is increased and flow rate of fluid flow increases.

4.9.1 Variation between different Aspect ratio and Temperature different

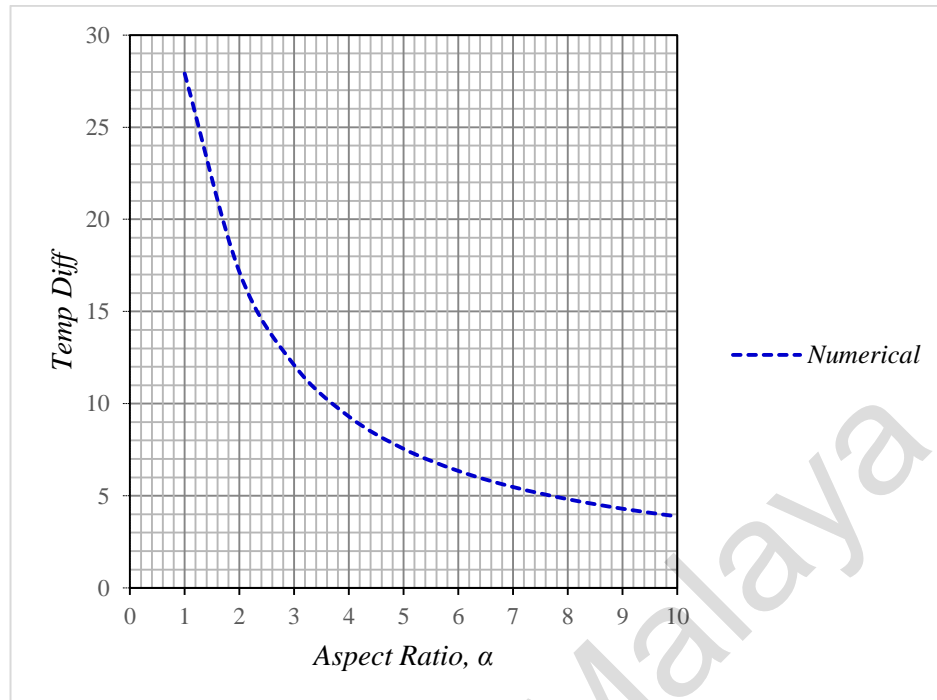


Figure 4.10: Temperature different of the microchannel for the different aspect ratio of the channel.

The main objective is to diminish the temperature variation of microchannel heat sink of the cooling system. The effects of aspect ratio on temperature different are shown in Figure 4.10. The temperature difference is calculated based on average wall and fluid temperature difference ($T_w - T_f$). From the Figure 4.10, it is observed that a high aspect ratio channel will enhance the contact surface area will results notable effects on the reduces temperature different of the heat sink temperature.

4.9.2 Variation between Aspect Ratio and Thermal Resistance

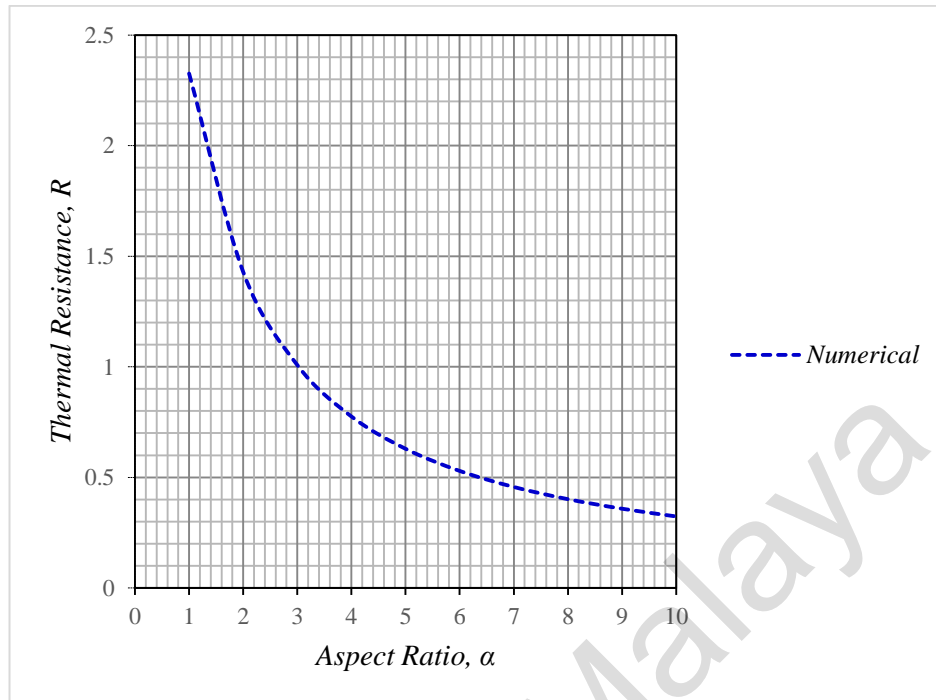


Figure 4.11: Total and spreading thermal resistance for the different aspect ratio of the channel.

At lowest aspect ratio, thermal resistances reach the peak and exponentially decrease when increasing aspect ratio as shown in Figure 4.11. At aspect ratios of 2, 4, and 6 thermal resistances is 1.428, 0.775, and 0.529 °C/W respectively. It showed 6% decrease of thermal resistance when the aspect ratio of channel varies from 1.0 to 10. At low aspect ratio, the thermal resistance is high when the flow rate is low and then decrease because the area of contact surface increase as the aspect ratio increases even if the flow rate is higher. Lower temperature different from the heat sink and significant increase in contact surface areas caused at higher aspect ratio channels the thermal resistance is lowest. However, the rate of change in thermal resistance is very negligible beyond certain aspect ratio (e.g., $\alpha = 8.0$), signifying the fact that infinite increase in height of channel does not produce enhancements on comparable heat transfer.

4.9.3 Variation between Aspect Ratio and Heat Transfer Coefficient

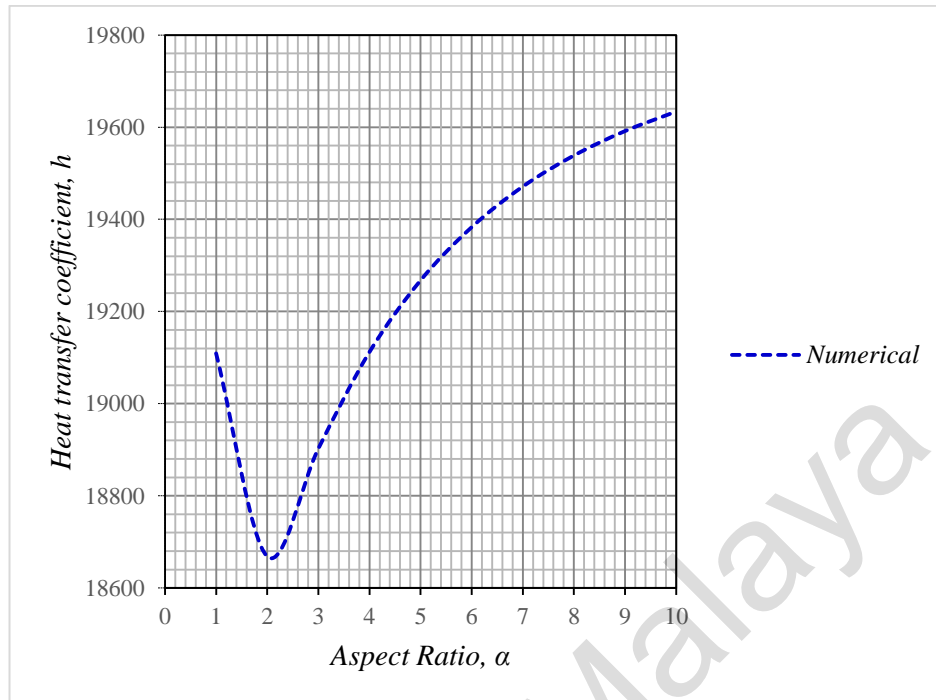


Figure 4.12: Heat transfer coefficient of the microchannel for the different aspect ratio of the channel.

The thermal performances of the heat sink depending on the convective heat transfer coefficient. Figure 4.12 shows the heat transfer coefficient at different aspect ratio. The coefficient of heat transfer is calculated based on the heat flux at the base surface per average wall and fluid temperature difference ($T_w - T_f$). Figure 4.12 emphasizes that there is an effective enhancement of the heat transfer coefficient in the range of aspect ratio of 1 to 10. At the highest aspect ratio, heat transfer coefficient gave around 19,634 W/m² then influence the heat transfer performance and increase the value of the Nusselt number of the heat sink. Besides that, the increases of Reynolds number also represent the improvement of the convective heat transportation capacity of the coolant and maximize the reduction of the base temperature of the heat sink.

4.9.4 Variation between Aspect Ratio and Nusselt number

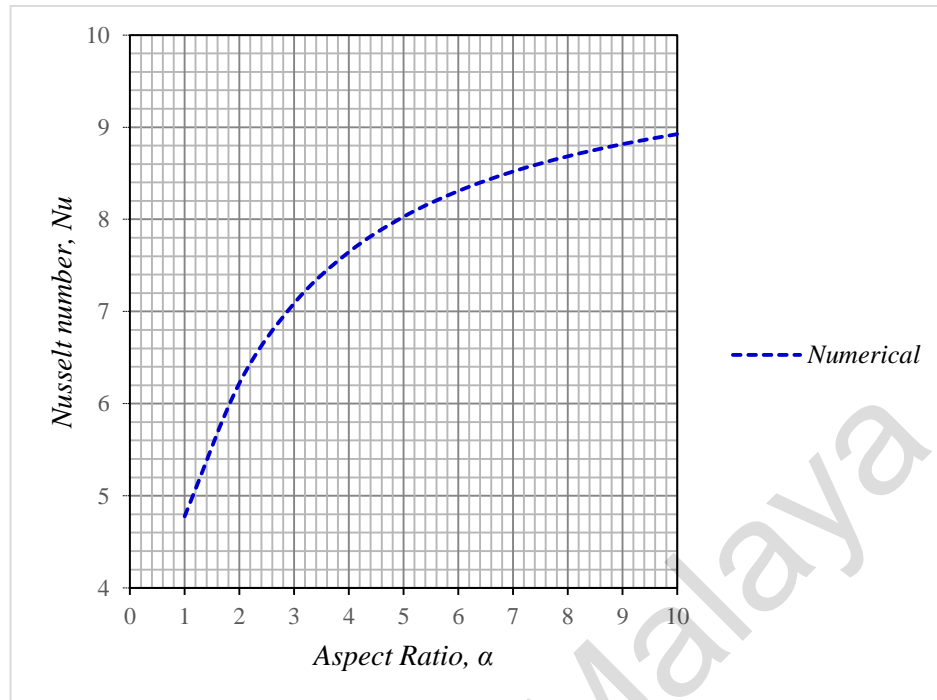


Figure 4.13: Fully developed average Nusselt number and different aspect ratios of the channel

Fully developed average Nusselt number (Nu) and different aspect ratio are demonstrated in Figure 4.13, which the Nusselt number is gradually increased with variation in aspect ratio. It is because of the larger aspect ratio of the channel, it will give the higher value of the Nusselt number and totally the contact surface will be larger and increase the heat transfer coefficient. As an example, if the size of the channel is 0.15mm (W) and 0.75mm (H), the aspect ratio will be based on $\alpha = H/W$ and will give a value of 5. At aspect ratios of 2, 4, and 6, the Nusselt number is 6.223, 7.645, and 8.306, respectively. The relationship between the fluid flow velocity and contact surface area of the channel influence in the Nusselt number and associated heat transfer coefficient at various aspect ratios.

4.9.5 Variation between different Aspect Ratio and Pressure Drop

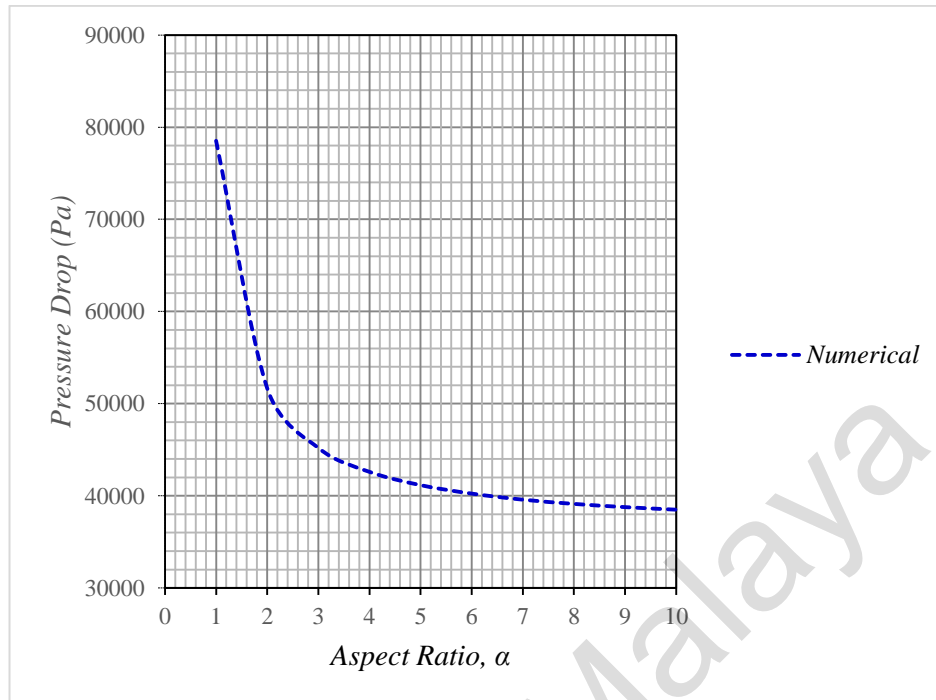


Figure 4.14: Relationship pressure drops of the microchannel for the different aspect ratio of the channel.

Pressure drop (ΔP) is corresponding to different aspect ratios are plotted in Figure 4.14. The pressure decreases from 78.52 to 38.5 kPa, when the aspect ratio of the channel increases from 1 to 10. A high pressure drops happened due to the higher flow rate accompanied with notable pressure drops across the microchannel heat sink for the low aspect ratio channels. Low fluid flow velocity caused pressure drop decrease as the channel aspect ratio increase. On the other hand, a higher aspect ratio of microchannel offers lower thermal and resistance lower pressure drop, however, the drawback is the contacting surface area has to be increased and thus more space is required for the heat sink.

4.9.6 Variation between different Aspect ratio and Pumping Power

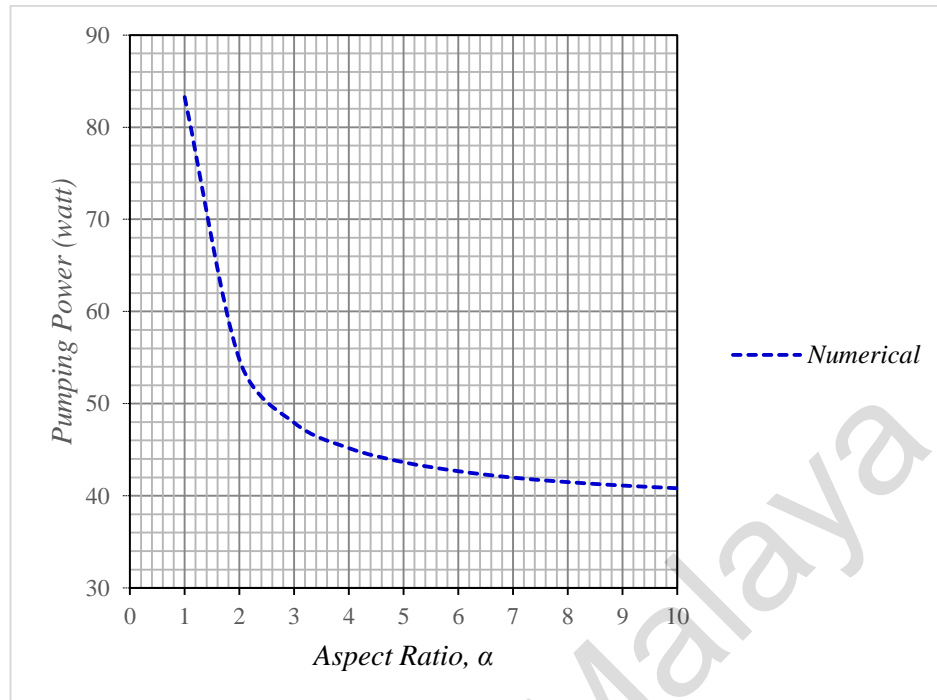


Figure 4.15: Relationship pumping power of the microchannel for the different aspect ratio of the channel.

The relationship between pumping power and different aspect ratio has been studied in order to identify the correlation between both. Based on Figure 4.15, the higher pumping power value will gradually reduce the value of aspect ratio of the channel. A pressure drop occurs when the coolant passes through the narrow channel of the heat sink. The system needs some extra pumping power to overcome this pressure drop. Figure 4.15 also demonstrates the decreasing in pumping power with the increasing in aspect ratio as well as cross-section area of fluid flow.

4.10 Effect of Flow rate

Similar to aspect ratio, the volume flow rates have been measured in this studied. The measured data of flow rates with different other parameters such as temperature different, thermal resistant, heat transfer coefficient, Nusselt number, pressure drop and pumping power are gathered by using numerical analysis. The similar data from (Sohel et al., 2014) was used to verify the flow characteristics of the microchannel. All the input parameters such as velocity, heat flux at the footprint, length and width of microchannels are kept constant. The heat source footprint is considered at $50 \text{ mm} \times 1.5 \text{ mm}$. The height of the channel, H is varied to obtain different aspect ratios (α) keeping the width of channel constant at $150 \text{ }\mu\text{m}$.

4.10.1 Variation between different Flow rate and Temperature Different

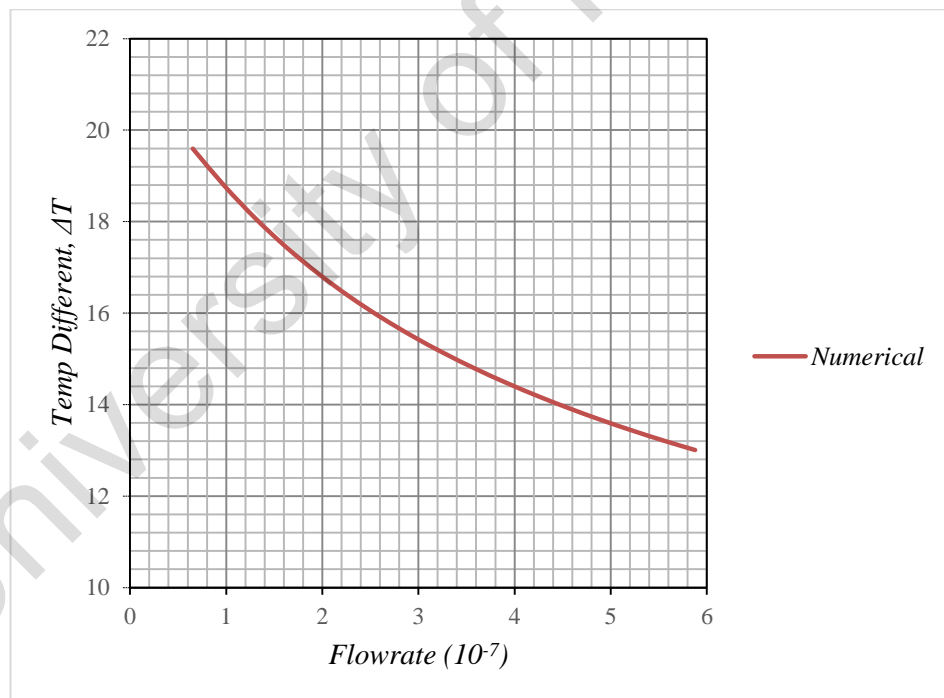


Figure 4.16: Temperature Different of the microchannel for the different flow rate of the channel.

The flow rate and temperature different of the straight channel were analyzed to have a clear picture of the fluid flow mechanism that causing the temperature different. The

variation between both is shown in Figure 4.16. It is found that total temperature different (ΔT) of the heat sink was reduced drastically from 19.5°C to 13°C with the increase of flow rate, hence with an increase of the fluid flow in the channel ultimately does not helps to absorb more heat from the solid body.

4.10.2 Variation between different Flow rate and Thermal Resistant

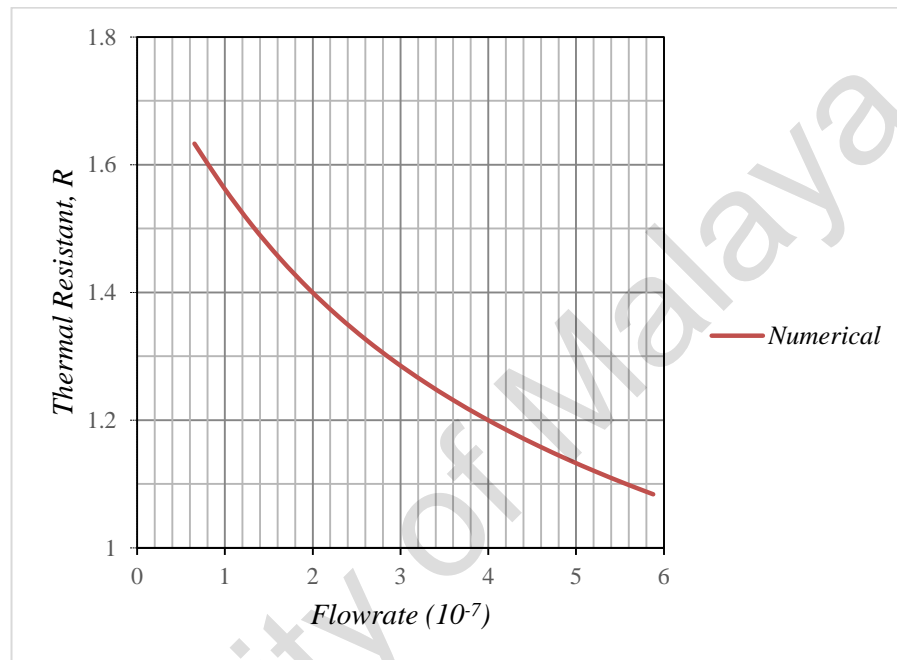


Figure 4.17: Thermal resistant of the microchannel for the different flow rate of the channel.

A similar trend is observed for variation between flowrate and thermal resistance, (R). Figure 4.17 portrays the trend of R with the variation of flow rate, it can be seen that total thermal resistance, R is decreased from $1.63^{\circ}\text{C}/\text{W}$ to $1.08^{\circ}\text{C}/\text{W}$ with the different variation of flow rate. With an increase in flow rate, a decrease in total thermal resistance is $0.55^{\circ}\text{C}/\text{W}$. As similar to temperature different, it can be said that with an increase the flow rate does not produce a significant reduction in thermal resistance.

4.10.3 Variation between different Flow rate and Heat Transfer Coefficient

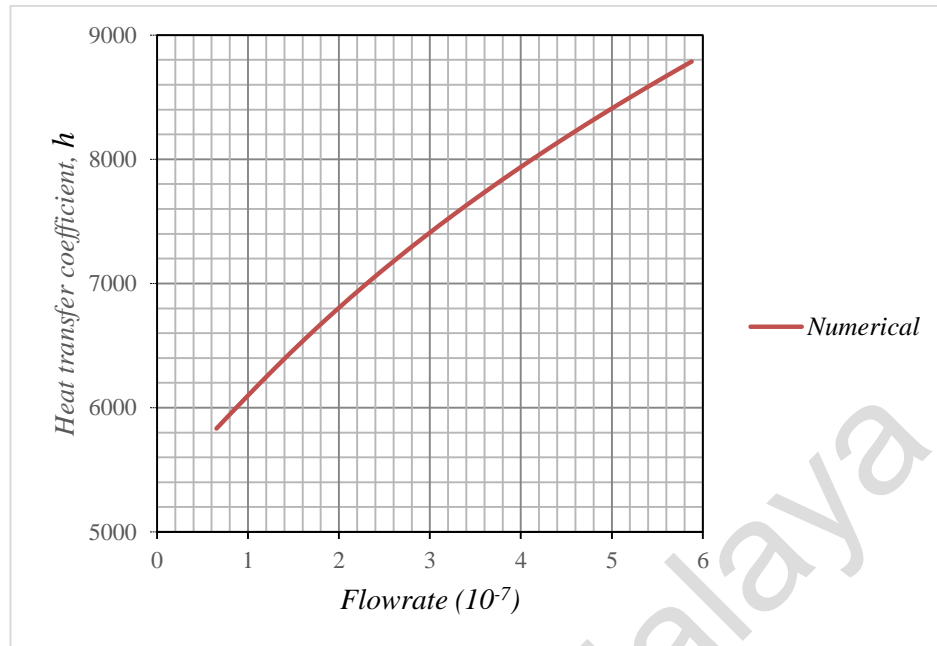


Figure 4.18: Heat transfer coefficient of the microchannel for the different flow rate of the channel.

Figure 4.18 demonstrates the trend variation between flowrate and heat transfer coefficient, (h). It shows that the increase in fluid flow or flow rate in the channel, the heat transfer coefficient enhances from 5,832 to 8,786 $W/(m^2 \cdot K)$. The higher value of heat transfer coefficient effected from this variation of flow rate will contribute to better of thermal performance of the microchannel heat sink.

4.10.4 Variation between different Flow rate and Nusselt number

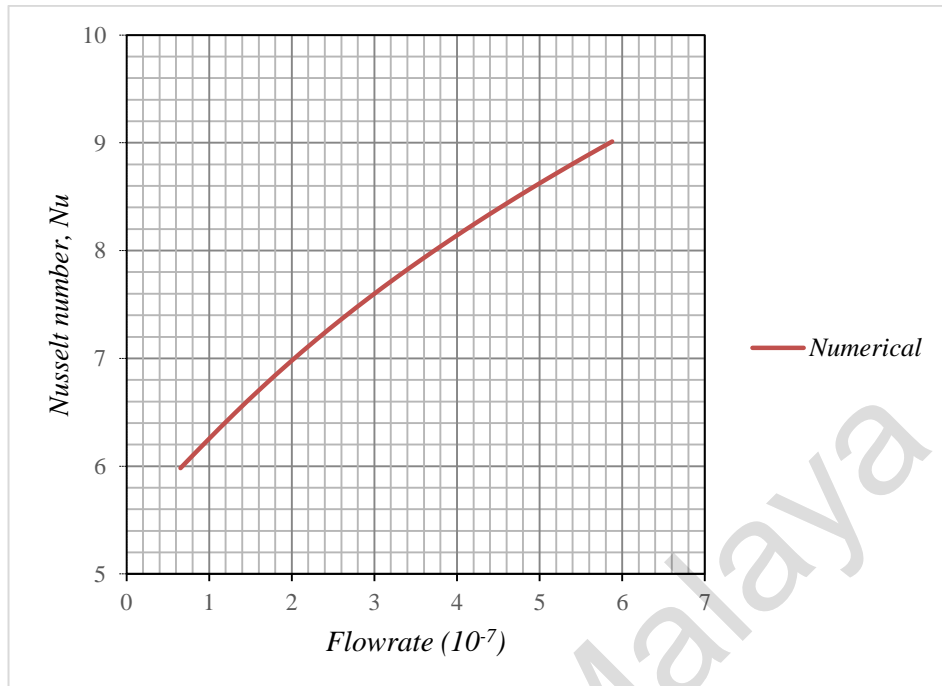


Figure 4.19: Fully developed Nusselt number and different flow rate

The evaluation of the thermal characteristic is performed based on the Nusselt number since heat transfer through advection is dominant. In the Figure 4.19, it is observed that Nusselt number tends to increase with increasing the value of flowrate. Generally, the Nusselt number (Nu) is the ratio of convective to conductive heat transfer across the boundary. It can be seen that the total Nusselt number gradually increase from 5.98 to 9.01 with the different variation of flow rate. The thermal performance of microchannel heat sink is depending on the Nusselt number which with a larger Nusselt number corresponds to more active convection and always accompanied by additional pressure drop.

4.10.5 Variation between different Flow rate and Pressure Drop

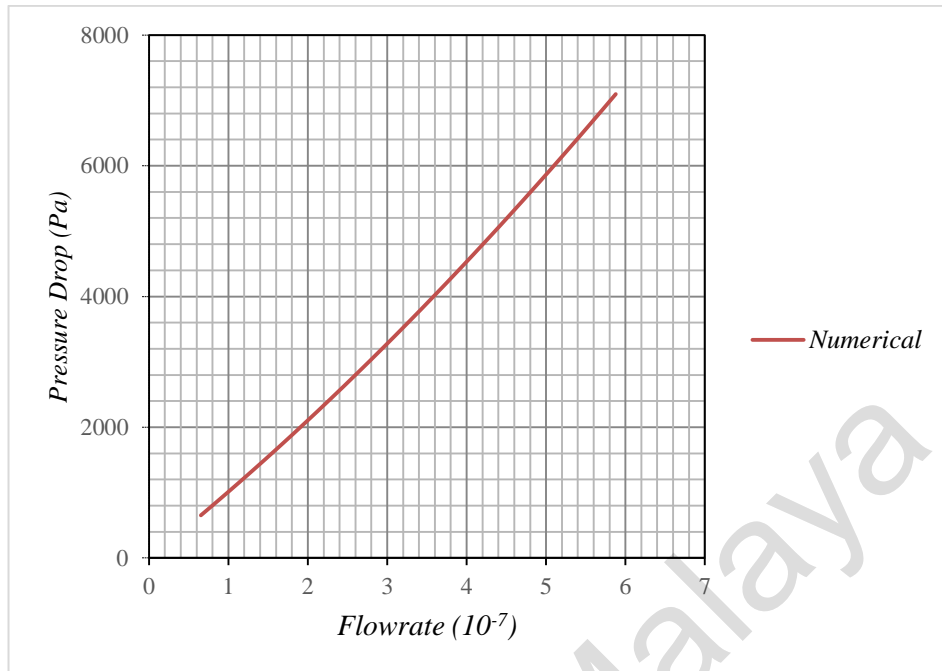


Figure 4.20: Pressure Drop of the microchannel for the different flow rate of the channel.

The total pressure drop (ΔP) is plotted in Figure 4.20 for different flow rates of the coolant. The total pressure drop of the heat sink channel rises from 652 to 7,096 Pa with the variation of flow rate. The effect of this variation of flow rate on the pressure drop will increase the friction in the channel. In Moody chart, the friction (f) in a straight channel will decrease as the laminar flow rate increases earlier than it reaches the transition zone. Apart from that, comparing the simple MCHS with increasing flow rate, the friction of the MCHS with passive enhancement will increase (Xia, Zhai, & Cui, 2013), (Kuppusamy, Mohammed, & Lim, 2013) and (Xia, Chai, Wang, Zhou, & Cui, 2011). Hence, the pressure drop does not reduce significantly with the increase of flow rate.

4.10.6 Variation between different Flow rate and Pumping Power

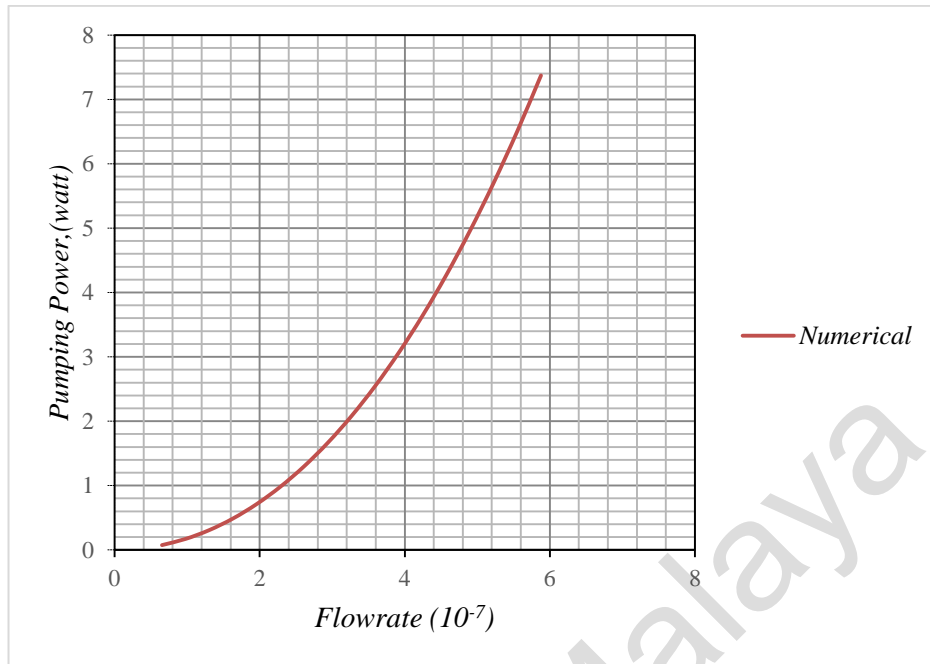


Figure 4.21: Pumping power of the microchannel for the different flow rate of the channel.

Figure 4.21 shows the trend of pumping power (W_{pp}) with different of flowrate for microchannel heat sink with the same hydraulic diameter ($D_h = 0.62\text{mm}$). It can be seen the value of pumping power increase gradually from 0.1 Watt to 7.3 Watt with the increasing number of flow rate. Relationships between pumping power and the fluid flow rate are really related to each other, this is because of the high pumping power normally will lead to higher water flow rate. In addition, the increased pressure drop also will lead to increase in pumping power.

CHAPTER 5: CONCLUSION AND RECOMMENDATION

5.1 Conclusions

This chapter focuses on validation of the thermal and hydraulic performance in a microchannel heat sink using the passive method and it was numerically investigated by predicting the thermal resistance, friction factor, Nusselt number and thermal enhancement. The study on the influence of different aspects ratio and fluid flow rate in the channel also presented. Results from the simulations can be summarized as follows:

- i. The numerical results conclude that straight MCHS can contribute better heat transfer enhancement with appropriate length and hydraulic diameter.
- ii. This study shows that the temperature increase along flow direction due to heat transfer from a lower wall with constant heat flux and it proved from this investigation the aluminum solid conducts more heat through the channel wall results temperature rise of water from 308K to 324K.
- iii. The hydraulic diameter (Dh) of the channel based on benchmark model with a constant velocity has predictable to absorb a lot of heat from heat source due to a larger surface area but it is shown that the existing Dh only able to absorb heat at both side wall and bottom which located nearest to the heat source. It can be concluded, the existing channel size or Dh can be reduced and it can be replaced with additional of the number of channels in order to increase the surface contact area of microchannel heat sink.
- iv. The study also shows that the pressure of coolant is increase as the distance of channel increases due to heat transfer occurs between wall and coolant in the microchannel. The current study observed that with using pure water as a cooling medium is assist to get lower pressure drop because of having lower viscosity.

- v. Based on the analytical and numerical analysis the validation result shows similar with the previous researcher, however, a proportional graph is slightly lower due to different hydraulic diameter and length of the channel used based on benchmark model which it will affect to the friction factor of the channel.
- vi. This study also shows that an increase initial surface contact area at the channel offers increased local convective heat transfer coefficient. The ratio between heat transfer by convection (α) and heat transfer by conduction alone (λ/L) is reduced when the distance of fluid flow is increased.
- vii. The validation based on numerical analysis and experimental shows that the results of the Poisseuille number (fRe) and Pressure drop (ΔP) against with Reynold number have a proportional graph but a slightly different on the experiment data due to surface roughness and fin edges collision in the microchannel. These showed that the numerical methods are highly feasible for implementation in practical applications.
- viii. Higher channel aspect ratio results in higher Nusselt number and heat transfer coefficient but lower temperature different, thermal resistance, pressure drop and pumping power.
- ix. Higher channel flow rate results in a higher Nusselt number, heat transfer coefficient, pressure drop and pumping power. However, higher of channel flow rate also will result in lower temperature different and thermal resistant.
- x. Finally, the required coolant flow rate and pressure drop can be reduced by using higher thermal conductivity heat sink materials, resulting in a smaller or cheaper pump required.

5.2 Recommendation for future works

There are some recommendations that could be made to improve the study of validation of the microchannel heat sink MCHS in the future:

- i. The current investigation conducted is based on the model validation and numerical solution is the benchmark at one researcher. The benchmark can be expanding to multiple researchers in order to get various validation data.
- ii. The validation of present numerical results is needed for such experimental work.
- iii. In other respects, more or further studies should be carried out with other volume concentration, base fluid and the combination of nanoparticles.

University of Malaysia

REFERENCES

- Anderson, G. and. (n.d.). Single-phase liquid friction factors in microchannels. *Thermal Sciences*.
- Bayazitoglu, J. F. T. and R. V. and Y. (2011). A Review of Cooling in Microchannels. *Heat Transfer Engineering*, 32.
- Choi, SB and Barron, R F and Warrington, R. (1991). Fluid flow and heat transfer in microtubes. *Asme Dsc*, 32, 123--134.
- Dhiman and A.K., and Choi, W.K. (2000). Experimental investigation of flow friction for liquid flow in microchannels. *Heat and Mass Transfer*, 27, 1165–1176.
- F. Peng, X & P. Peterson, G & X. Wang, B. (1994). Heat Transfer Characteristics of Water Flowing Through Microchannels. *Experimental Heat Transfer - EXP HEAT TRANSFER.*, 7, 265–283.
- Hestsroni, R., Laser, D., Zhou, P., Asheghi, M., Devasenathipathy, S., Kenny, T., Santiago, J., and Goodson, K. (2000). EXPERIMENTAL INVESTIGATION OF FLOW TRANSITION IN MICROCHANNELS USING MICRON RESOLUTION PARTICLE IMAGE VELOCIMETRY. *Thermomechanical Phenomena in Electronic Systems Proceedings of the Intersociety Conference*, 2, 148–153.
- Judy, Cheng, yal, Maynes, D., andWebb, B.W. (2002). Characterization of frictional pressure drop for liquid flows through microchannels. *Heat and Mass Transfer*, 45, 3477–3489.
- Judy, J., Maynes, D., & Webb, B. W. (2002). Characterization of frictional pressure drop for liquid flows through microchannels. *International Journal of Heat and Mass Transfer*, 45(17), 3477–3489. [https://doi.org/10.1016/S0017-9310\(02\)00076-5](https://doi.org/10.1016/S0017-9310(02)00076-5)
- K ambiz, K.V., and Adrian, R.J. (2004). Transition from laminar to turbulent flow in liquid filled microtubes. *Experiment in Fluids*, 36, 741–747.
- Kohl, M. J., Abdel-Khalik, S. I., Jeter, S. M., & Sadowski, D. L. (2005). An experimental investigation of microchannel flow with internal pressure

measurements. *International Journal of Heat and Mass Transfer*, 48(8), 1518–1533. <https://doi.org/10.1016/j.ijheatmasstransfer.2004.10.030>

Kuppusamy, N. R., Mohammed, H. A., & Lim, C. W. (2013). Numerical investigation of trapezoidal grooved microchannel heat sink using nanofluids. *Thermochimica Acta*, 573, 39–56. <https://doi.org/10.1016/j.tca.2013.09.011>

Lee, S.Y., Wereley, Hetsroni, Gui, W., and Mudawar, I. (2002). Microchannel flow measurement using micro particle image velocimetry. *Asme*, 258, 493–500.

Li, H., Ewoldt, R., & Olsen, M. G. (2005). Turbulent and transitional velocity measurements in a rectangular microchannel using microscopic particle image velocimetry. *Experimental Thermal and Fluid Science*, 29(4), 435–446. <https://doi.org/10.1016/j.expthermflusci.2004.06.001>

Li, H., & Olsen, M. G. (2006). Aspect Ratio Effects on Turbulent and Transitional Flow in Rectangular Microchannels as Measured With MicroPIV. *Journal of Fluids Engineering*, 128(2), 305. <https://doi.org/10.1115/1.2170122>

Liu, Dong and Garimella, S. V. (2004). Investigation of Liquid Flow in Microchannels. *Journal of Thermophysics and Heat Transfer*, 18, 65--72.

Peng, X. F., & Peterson, G. P. (1995). The effect of thermofluid and geometrical parameters on convection of liquids through rectangular microchannels. *International Journal of Heat and Mass Transfer*, 38(4), 755–758. [https://doi.org/10.1016/0017-9310\(95\)93010-F](https://doi.org/10.1016/0017-9310(95)93010-F)

Pfund, David and Rector, David and Shekarriz, Alireza and Popescu, Aristotel and Welty, J. (2000). Pressure drop measurements in a microchannel. *AIChE Journal*, 46(1547–5905), 1496--1507.

Phillips, R. J. (1988). Microchannel heat sinks. *Lincoln Lab. J*, 1, 31--48.

Poh, S. T., & Ng, E. Y. K. (1998). Heat transfer and flow issues in manifold microchannel heat sinks: a CFD approach. *Proceedings of 2nd Electronics Packaging Technology Conference (Cat. No.98EX235)*, 246–250. <https://doi.org/10.1109/EPTC.1998.756010>

- Qu, W., & Mudawar, I. (2002). Experimental and numerical study of pressure drop and heat transfer in a single-phase micro-channel heat sink. *International Journal of Heat and Mass Transfer*, 45(12), 2549–2565. [https://doi.org/10.1016/S0017-9310\(01\)00337-4](https://doi.org/10.1016/S0017-9310(01)00337-4)
- Rahman, M. M. (2000). Measurements of heat transfer in microchannel heat sinks. *International Communications in Heat and Mass Transfer*, 27(4), 495–506. [https://doi.org/10.1016/S0735-1933\(00\)00132-9](https://doi.org/10.1016/S0735-1933(00)00132-9)
- Rahman, M. M., & Gui, F. (1993). Experimental measurements of fluid flow and heat transfer in microchannel cooling passages in a chip substrate. *The ASME International Electronics Packaging Conference, Binghamton, NY, USA, 09/29-10/02/93*, 685–692.
- Raja Kuppusamy, N. (2016). *Thermal Enhancement of Microchannel Heat Sink Using Passive Method*. Universiti of Malaya.
- Rodgers. (2003). An experimental study of convective heat transfer in silicon microchannels with different surface conditions. *Heat and Mass Transfer*, 46, 2547–2556.
- Roy and Aet. (2002). Experimental and numerical study of pressure drop and heat transfer in a single phase microchannel heat sink. *Heat and Mass Transfer*, 45, 2549–2565.
- Setal, K. and. (2004). Investigation of liquid flow in microchannels. *Thermophysics and Heat Transfer*, 18, 65–72.
- Sobhan, Choondal B and Garimella, S. V. (2001). A comparative analysis of studies on heat transfer and fluid flow in microchannels. *Microscale Thermophysical Engineering*, 5, 293--311.
- Sohel, M. R., Khaleduzzaman, S. S., Saidur, R., Hepbasli, A., Sabri, M. F. M., & Mahbulul, I. M. (2014). An experimental investigation of heat transfer enhancement of a minichannel heat sink using Al₂O₃-H₂O nanofluid. *International Journal of Heat and Mass Transfer*, 74, 164–172. <https://doi.org/10.1016/j.ijheatmasstransfer.2014.03.010>

- Sohel, M. R., Saidur, R., Sabri, M. F. M., Kamalisarvestani, M., Elias, M. M., & Ijam, A. (2013). Investigating the heat transfer performance and thermophysical properties of nanofluids in a circular micro-channel. *International Communications in Heat and Mass Transfer*, 42, 75–81. <https://doi.org/10.1016/j.icheatmasstransfer.2012.12.014>
- Steinke, Mark E. Kandlikar, S. G. (2005). Single-Phase Liquid Heat Transfer in Microchannels. *ASME 3rd International Conference on Microchannels and Minichannels*, 667–678.
- Steinke, M. E., & Kandlikar, S. G. (2006). Single-phase liquid friction factors in microchannels. *International Journal of Thermal Sciences*, 45(11), 1073–1083. <https://doi.org/10.1016/j.ijthermalsci.2006.01.016>
- Tuckerman, D. B. (1984). Heat-Transfer Microstructures for Integrated Circuits. *Ph.D. Thesis*, (February), 141.
- Tuckerman, D. B., & Pease, R. F. W. (1981). High-performance heat sinking for VLSI. *IEEE Electron Device Letters*, 2(5), 126–129. <https://doi.org/10.1109/EDL.1981.25367>
- Wu, P., & Little, W. A. (1984). Measurement of the heat transfer characteristics of gas flow in fine channel heat exchangers used for microminiature refrigerators. *Cryogenics*, 24(8), 415–420. [https://doi.org/10.1016/0011-2275\(84\)90015-8](https://doi.org/10.1016/0011-2275(84)90015-8)
- Xia, G., Chai, L., Wang, H., Zhou, M., & Cui, Z. (2011). Optimum thermal design of microchannel heat sink with triangular reentrant cavities. *Applied Thermal Engineering*, 31(6–7), 1208–1219. <https://doi.org/10.1016/j.applthermaleng.2010.12.022>
- Xia, G., Zhai, Y., & Cui, Z. (2013). Numerical investigation of thermal enhancement in a micro heat sink with fan-shaped reentrant cavities and internal ribs. *Applied Thermal Engineering*, 58(1–2), 52–60. <https://doi.org/10.1016/j.applthermaleng.2013.04.005>
- Zeighami, R., Laser, D., Zhou, P., Asheghi, M., Devasenathipathy, S., Kenny, T., ... Goodson, K. (2000). Experimental investigation of flow transition in microchannels using micron-resolution particle image velocimetry, 2, 148–153

Zhang, HY and Pinjala, D and Iyer, MK and Nagarajan, R and Joshi, YK and Wong, TN and Toh, K. (2005). Assessments of single-phase liquid cooling enhancement techniques for microelectronics systems. *Proc. ASME/Pacific Rim Technical Conference and Exhibition on Integration and Packaging of MEMS, NEMS, and Electronic Systems: Advances in Electronic Packaging*, 17--22.

Zhi-Xin Li. (2003). EXPERIMENTAL STUDY ON FLOW CHARACTERISTICS OF LIQUID IN CIRCULAR MICROTUBES. *Microscale Thermophysical Engineering*, 7(3), 253–265.

University of Malaya